

Consortium



for

Small-Scale Modelling

# *Newsletter*

*August 2008*

*No. 8*

Deutscher  
Wetterdienst

MeteoSwiss

Ufficio Generale Spacio  
Aero e Meteorologia

Instytucie Meteorologii i  
Gospodarki Wodnej

Agenzia Regionale per la  
Protezione Ambientale dell  
Piemonte

Centro Italiano Ricerche  
Aerospaziali



ΕΘΝΙΚΗ  
ΜΕΤΕΩΡΟΛΟΓΙΚΗ  
ΥΠΗΡΕΣΙΑ

Administratia Nationala de  
Meteorologie

Agenzia Regionale per la Protezione  
Ambientale dell Emilia-Romagna:  
Servizio Idro Meteo

Amt für GeoInformationswesen  
der Bundeswehr

[www.cosmo-model.org](http://www.cosmo-model.org)

Editors: Ulrich Schättler (DWD); Andrea Montani (ARPA-SIM); Massimo Milelli (ARPA Piemonte)  
Printed at Deutscher Wetterdienst, P.O. Box 100465, 63004 Offenbach am Main



---

**Table of Contents**

<b>Editorial</b>	<b>1</b>
Introduction	
<i>Ulrich Schättler</i> . . . . .	1
<b>3 Working Group on Physical Aspects</b>	<b>2</b>
TKE as a Measure of Turbulence	
<i>B. Szintai, P. Kaufmann</i> . . . . .	2
An Advanced Snow Parameterization for Models of Atmospheric Circulation	
<i>E. Machul'skaya, V. Lykosov</i> . . . . .	10
Revision of the Turbulent Gust Diagnostics in the COSMO-Model	
<i>J.-P. Schulz</i> . . . . .	17
<b>4 Working Group on Interpretation and Applications</b>	<b>23</b>
Five Years of Limited-Area Ensemble Activities at ARPA-SIM: The COSMO-LEPS System	
<i>A. Montani, C. Marsigli, T. Paccagnella</i> . . . . .	23
The COSMO-SREPS Priority Project: The Autumn 2008 Testing Period	
<i>C. Marsigli, A. Montani, T. Paccagnella, F. Gofa, P. Louka</i> . . . . .	27
<b>5 Working Group on Verification and Case Studies</b>	<b>37</b>
Report about the Latest Results of Precipitation Verification over Italy	
<i>E. Oberto, M. Turco</i> . . . . .	37
High Resolution Verification of COSMO-I7 2m Temperature over Emilia-Romagna Region	
<i>M.-S. Tesini, C. Cacciamani</i> . . . . .	45
<b>Appendix: List of COSMO Newsletters and Technical Reports</b>	<b>57</b>

## 1 Introduction

The contributions to this Newsletter are summaries from the presentations given by COSMO staff during the 9<sup>th</sup> General Meeting in Athens (from 18.-21. September 2007). There are only few contributions this time, which may result from the fact, that most Priority Projects were just about to end, and a final report could not yet be given or will be prepared as a COSMO Technical Report in the near future.

We know that writing documentations and contributions for a Newsletter or a Technical Report always is an imposition to scientists. And that the Newsletters are always published long time after the meetings does not help in this matter. Therefore we welcome the support we will get in the next COSMO year by our colleagues from Romania, who take over the editor work for the COSMO Newsletter. We kindly ask all scientists, to support the new editors by submitting their contributions in time and according to the latex-template. And we want to thank all authors for the (hopefully) fruitful collaboration in the last years

Ulrich Schättler  
Andrea Montani  
Massimo Milelli

Ulrich.Schaettler@dwd.de  
amontani@arpa.emr.it  
Massimo.Milelli@arpa.piemonte.it



Figure 1: Participants of the 9th COSMO General Meeting in Athens

## TKE as a Measure of Turbulence

BALÁZS SZINTAI, PIRMIN KAUFMANN

*MeteoSwiss, Krähbühlstrasse 58, 8044 Zürich, Switzerland*

### 1 Introduction

MeteoSwiss is using an integrated modelling system to simulate the dispersion of radioactive materials in emergency situations. For the prediction of the atmospheric flow, the COSMO numerical weather prediction model (Doms and Schättler, 2002) is used, which is run operationally at two horizontal resolutions at MeteoSwiss. COSMO-7 has a horizontal resolution of 6.6 km and is integrated out to 72 hours twice a day on a European domain, while COSMO-2, which is nested in COSMO-7, has a 2.2 km horizontal resolution and provides 24 hour forecasts eight times a day for a smaller domain covering Switzerland. Until December 2005 the COSMO model applied a first order closure for subgrid scale turbulence (level 2 in the Mellor and Yamada notation), which was upgraded to a one-and-a-half order (level 2.5) closure with a prognostic equation for turbulent kinetic energy (TKE) (Mellor and Yamada, 1982). Both COSMO-7 and COSMO-2 are coupled off-line with the Lagrangian Particle Dispersion Model (LPDM, Glaab et al., 1998) with hourly input meteorological data. The two models use the same grid, consequently, no grid transformation is required.

### 2 Turbulence coupling with the COSMO model

#### 2.1 Coupling approaches

According to the above mentioned turbulence closure versions of the COSMO model, the coupling of the COSMO model with LPDM can be performed in three different ways. The first coupling type uses first order closure in the COSMO model, and the turbulence statistics (mainly TKE and eddy diffusivities) are post-diagnosed in LPDM with the same closure assumptions. In the second coupling type the COSMO model uses the new closure with prognostic TKE, but the turbulence statistics are still post-diagnosed in the dispersion model, while in the third type the prognostic TKE of the COSMO model is used directly by LPDM. These different coupling types resulted in highly different concentrations during the investigated case studies.

In these experiments, an imaginary radioactive emission was modelled with the COSMO-7–LPDM system on a European domain for 48 hours. The case studies covered different synoptic situations and the most pronounced differences between the coupling types were detected in the case with strong cyclonic activity (23 October 2006). In this case the modelled pollutant cloud showed similar characteristics with the first and third coupling type, while the second type resulted in a more dispersed cloud with smaller maximums (Fig. 1 upper panel).

During the investigation of the turbulence statistics in the dispersion model it turned out, that these differences are caused by highly different TKE values (Fig. 1 lower panel). With the second coupling type, much higher TKE values were detected, compared to those with the first and third type; differences could reach a factor of 10 on areas with strong cyclonic activity.

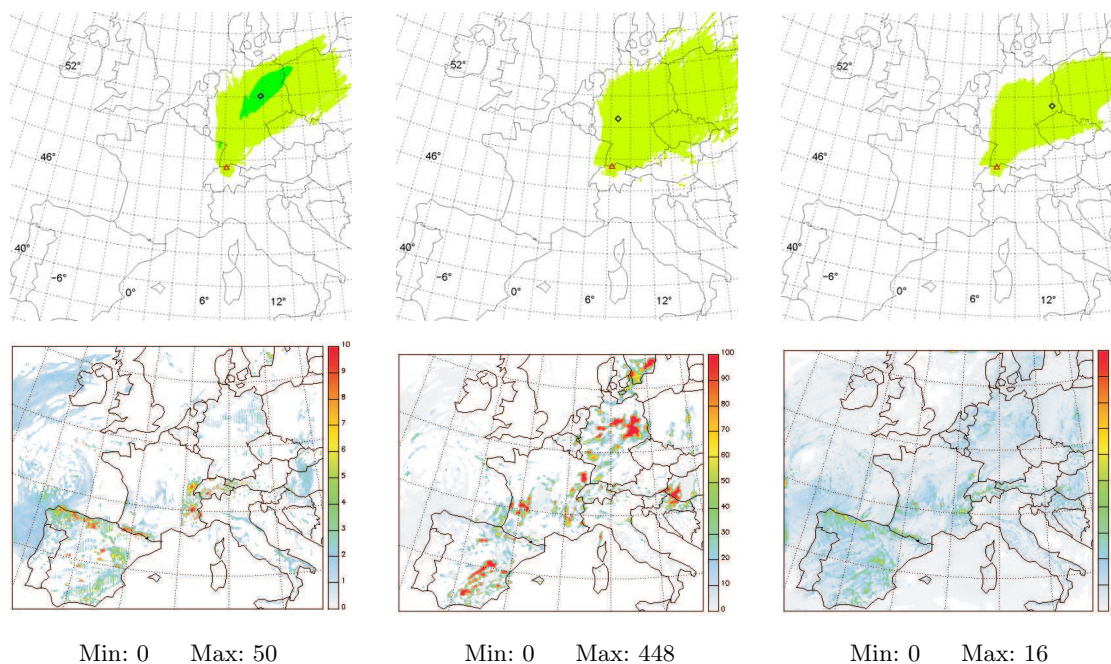


Figure 1: Concentration calculations (upper panel) and the corresponding TKE values (lower panel) from the dispersion model for the case study of 23 October 2006. TKE values at level 41 ( $\sim 460$  m AGL) are shown. The three different coupling types from left to right: COSMO with diagnostic TKE, post-diagnosed by LPDM; COSMO with prognostic TKE, post-diagnosed by LPDM; COSMO with prognostic TKE, direct usage of TKE by LPDM. Note that the color-scaling of the TKE plot in the case of the second coupling type indicates higher values by a factor of 10.

These results show that the mean meteorological fields of the COSMO model are more dependent on the turbulence closure than it was previously expected. This dependency gets most pronounced if the turbulence characteristics are post-diagnosed by the dispersion model using different closure assumptions, as it has been done in the case of the second coupling type. However, if the turbulence parametrizations of the two models are consistent (first order in the first type, one-and-a-half order in the third type), more realistic TKE values are present in the dispersion model. Consequently, when coupling dispersion models to the COSMO model, always the same type of turbulence closure should be used in the two models.

## 2.2 TKE oscillations

Further investigation of COSMO model outputs revealed occasional unrealistic oscillations in the TKE profiles. These oscillations were discovered mainly in stably stratified situations and are considered to be a result of numerical instability in the diffusion scheme. In Fig. 2 forecasted vertical profiles from the COSMO model are shown for a grid point located over northern Switzerland. Comparing the profiles of the different variables it can be concluded that the TKE oscillations have an impact on the mean meteorological variables, as some unrealistic wiggles appear in the wind and temperature profiles as well. The magnitude of these features in the mean variables are apparently small. However, if TKE is post-diagnosed in the dispersion model from the vertical gradients of the mean variables (second coupling type), highly unrealistic TKE values are obtained (Fig. 2, lower right panel).

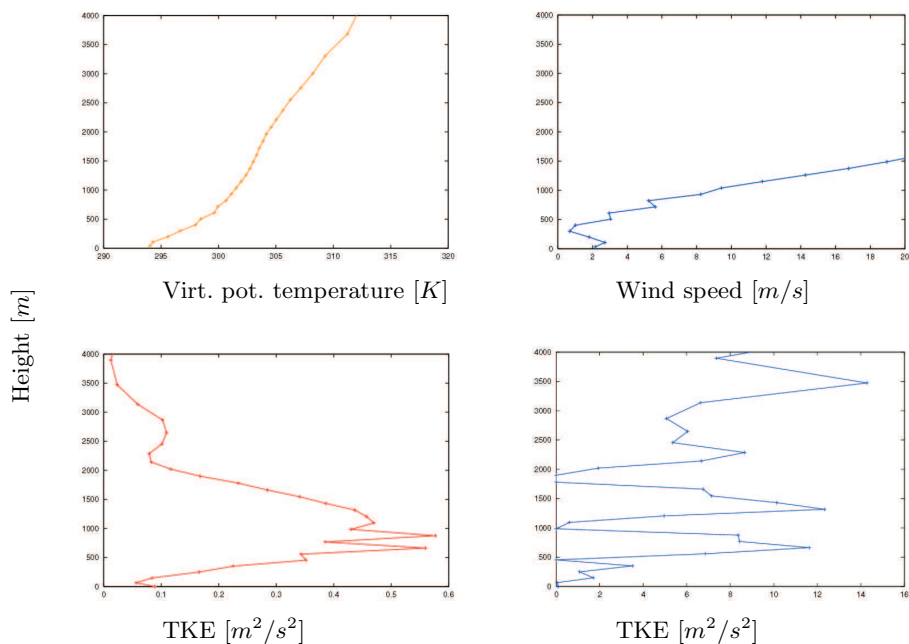


Figure 2: Forecasted vertical profiles for a grid point located over northern Switzerland on 23 October 2006 at 12 UTC. 12 hour COSMO forecast of: virtual potential temperature [K] (upper left), wind speed [m/s] (upper right) and TKE [m<sup>2</sup>/s<sup>2</sup>] (lower left). In the lower right panel the post-diagnosed TKE values from LPDM are showed.

It has to be noted, that for the above described experiment the Leapfrog time integration scheme has been used. Repeating the experiment with the Runge-Kutta scheme (which is operational at MeteoSwiss since November 2007) the above mentioned TKE oscillations are of smaller amplitudes.

### 3 Boundary layer height determination

Results shown above imply that TKE is a rather important input variable for a Lagrangian particle dispersion model. However, TKE is not a conventional model variable and it is not verified routinely like temperature, wind or humidity. Consequently, there is a certain demand from the point of dispersion applications to achieve a better understanding of the currently used turbulence scheme and to try to validate the turbulence variables of the COSMO model in different situations. For this reason, an experiment is planned at MeteoSwiss, which aims at the intercomparison of turbulence characteristics of the COSMO model with measurements, LES data and scaling considerations. To be able to use similarity theory approaches for the determination of dispersion parameters, first the height of the planetary boundary layer (PBL) has to be determined from COSMO model outputs. In the following different methods which were applied to COSMO model outputs for PBL height determination will be discussed and results concerning their validation will be shown.

### 3.1 Methodology

At MeteoSwiss methods using the following characteristics were applied to COSMO model fields to diagnose the height of the PBL:

- Bulk Richardson number
- Gradient Richardson number
- TKE
- Momentum and heat fluxes
- Theoretical approaches based on surface fluxes

By calculating the bulk Richardson number ( $Ri_b$ ) the diagnosed 2 m temperature was used as a reference and the no-slip condition was applied (i.e. reference wind was 0). According to the literature a critical  $Ri_b$  of 0.22 (Vogelenzang and Holtslag, 1996) was used for unstable conditions and a critical value of 0.33 (Wetzel, 1982) in stable situations. By using the gradient Richardson number a critical value of 0.38 was applied. In both cases the top of the PBL was defined as the first height where the critical value of the Richardson number was reached.

When using TKE for PBL height determination, first the maximum value of TKE was searched in a predefined lower part of the atmosphere (2000 m for unstable and 500 m for stable conditions), and the critical TKE value ( $TKE_c$ ) was defined with a certain threshold ( $th$ ):  $TKE_c = TKE_{max} * th$ . During the evaluation different threshold values were tested for stable and unstable stratification. For the momentum fluxes the same methodology was used, however, always the surface momentum flux was used as a reference to calculate the critical value. The PBL top was then determined at the height where TKE or the momentum flux first dropped below the critical value. When using the heat flux of the model the PBL height was determined as the level of the heat flux minimum.

Theoretical approaches to determine the PBL height have also been implemented. These methods are based on the surface heat and momentum fluxes and the background stratification above the PBL. For the convective boundary layer the slab model equation of Batchvarova and Gryning (1991) was used to calculate the growth rate of the boundary layer:

$$\frac{dh}{dt} = (1 + 2A) \frac{Q_0}{\gamma_\theta h} + 2B \frac{u_*^3}{\gamma_\theta \beta h^2},$$

where  $h$  is the PBL height,  $Q_0$  is the surface potential temperature flux,  $u_*$  is the friction velocity,  $\beta$  is the buoyancy parameter,  $\gamma_\theta$  is the background stratification above the PBL and  $A$  and  $B$  are model constants. The integration of the above equation was started at sunrise, when the surface sensible heat flux becomes positive, and it was initiated with a PBL height of 50 m.

For the height of the stable boundary layer the diagnostic equation of Zilitinkevich et al. (2007) was applied:

$$\frac{1}{h^2} = \frac{f^2}{(C_R u_*^2)^2} + \frac{N|f|}{(C_{CN} u_*^2)^2} + \frac{|f\beta Q_0|}{(C_{NS} u_*^2)^2},$$

where  $f$  is the Coriolis parameter,  $N$  is the Brunt-Väisälä frequency and  $C_R$ ,  $C_{CN}$  and  $C_{NS}$  are empirical constants.

### 3.1 Validation

The PBL heights determined by the above mentioned methods were validated against radiosoundings in stable and unstable situations. Ten stable and ten convective days were chosen in 2006 and 2007. On each day the PBL height methods were validated against ten radiosounding stations, consequently, the present study is based on approximately 100 cases regarding both stable and unstable situations. The following stations were chosen to cover most of the COSMO-7 domain: Essen, Idar, Lindenberg, Lyon, Milan, Munich, Payerne, Stuttgart, Trappes and Vienna.

To determine the boundary layer height objectively from the radiosoundings, the bulk Richardson number was applied for the measured virtual potential temperature and wind profiles. For convective days a critical  $Ri_b$  of 0.22 was used, which turned out to be a reliable measure and showed good agreement with the subjectively defined PBL top. For stable days a critical  $Ri_b$  of 0.33 was applied, which value worked well for well mixed stable boundary layers with an elevated inversion. However, especially in the case of radiation dominated stable boundary layers this method often failed to determine a realistic PBL height. In these cases  $Ri_b$  exceeded the critical value already at the first measurement level. If this happened, then starting from the surface the first height was searched, where the potential temperature profile was "close" to adiabatic, i.e. the potential temperature gradient was smaller than 0.72 K/100 m. The combination of these two methods showed reasonable agreement with the subjectively defined PBL top, however, to achieve a more robust method to determine PBL height objectively in stable situations is still an unresolved problem.

PBL heights determined from the radiosoundings were compared to 12 hour forecasts of the COSMO model during the above mentioned stable and convective days. In the experiments the model version 4.0.4 was used. Both horizontal resolutions of the COSMO model were tested, namely, COSMO-7 with 7 km horizontal resolution and 45 vertical levels and COSMO-2 with 2.2 km horizontal resolution and 60 vertical levels. COSMO-7 was initialized from its own assimilation cycle, while the initial conditions for COSMO-2 were interpolated from the COSMO-7 analysis due to the fact that in 2006 no assimilation cycle was running at MeteoSwiss for COSMO-2. The PBL height determination methods were applied for the COSMO model to the grid point which was closest to the radiosounding location. For the verification different scores (bias, standard deviation, RMSE) were calculated and scatter plot diagrams were analyzed.

Table 1: Verification scores for convective cases. Absolute and relative biases, standard deviation of errors and root mean square error (absolute and relative). For the different methods the critical values or thresholds are indicated in parantheses.

	<b>Ri</b> <b>(0.38)</b>	<b>TKE</b> <b>(0.1)</b>	<b>Mom. Fl.</b> <b>(0.1)</b>	<b>Heat Fl.</b> <b>(min)</b>	<b>Slab</b> <b>model</b>	<b>Bulk Ri</b> <b>(0.22)</b>
<b>BIAS (m)</b>	-775.4	-512.4	-561.4	-626.5	-2	526.7
<b>BIAS-rel</b>	-0.442	-0.24	-0.288	-0.359	0.09	0.441
<b>STDEV (m)</b>	493	556.9	518.4	684.5	560.9	802
<b>RMSE (m)</b>	791	613.2	626.1	782.7	401.1	675.9
<b>RMSE-rel</b>	0.465	0.366	0.377	0.464	0.297	0.519

Table 1 shows verification scores for the different methods applied to COSMO-7 forecasts during convective cases. The slab model performs very well with practically no bias, the bulk Richardson number method shows strong positive bias, while the other methods negative biases with the largest underestimation in the case of the gradient Richardson number. The scatter of the errors is considerably large by all the methods. Concerning the root mean square error the slab model is the best followed by the methods based on TKE and momentum fluxes.

Figure 3 shows the dependence of model errors on the observed PBL height. With every method – except the bulk Richardson number method – the same features can be observed, namely, the shallower ( $\sim 700$  m) boundary layers are overestimated, while the higher ( $\sim 2500$  m), well-developed boundary layers are underestimated by the COSMO model. To understand this problem, model forecasts for the station of Lindenberg were investigated in more details. For this station extensive measurement data was available, including soil moisture measurements. The underestimation of well-developed PBLs could be caused by a too moist soil compared to measurements in the COSMO analysis. This high soil moisture leads to overestimated latent and underestimated sensible surface heat fluxes, and consequently a too moist and under-developed boundary layer (Fig. 4). For convective days PBL height results from the COSMO-2 model do not show significant differences from the results of COSMO-7. This could be caused by the fact, that the investigated convective cases showed great sensitivity towards the soil moisture, which was similar in the two models due to the common analysis used.

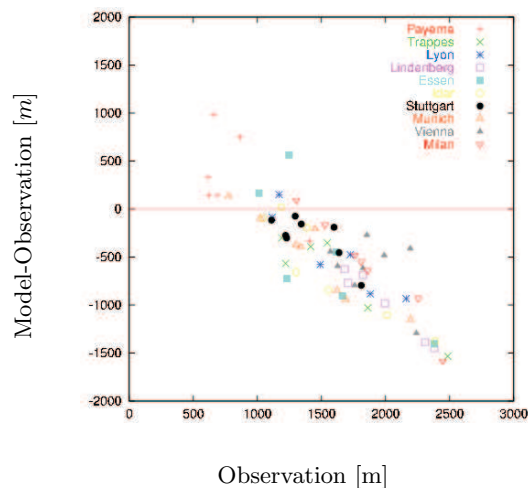


Figure 3: Scatter plot diagram of the determined PBL heights from 12 hour COSMO-7 forecasts. On the y-axis the model errors are depicted. Results of the TKE-method (with a 10% threshold) are shown for convective days.

For stable days the same methods were investigated as for convective cases, however, with somewhat higher thresholds. Both with the TKE and momentum flux method a threshold of 20% proved to be the most appropriate, in contrast to the 10% threshold used during unstable days. The use of higher thresholds was necessary due to a known problem of the COSMO model in stable situations. As a minimum turbulent diffusion coefficient of  $K_{min} = 1 \text{ m}^2/\text{s}$  is applied in the COSMO model, it causes the very stable boundary layer to be more active than in reality, and consequently higher thresholds are needed to find a suitable PBL top in the model.

While during convective days usually all the methods were successful in finding a PBL top, it

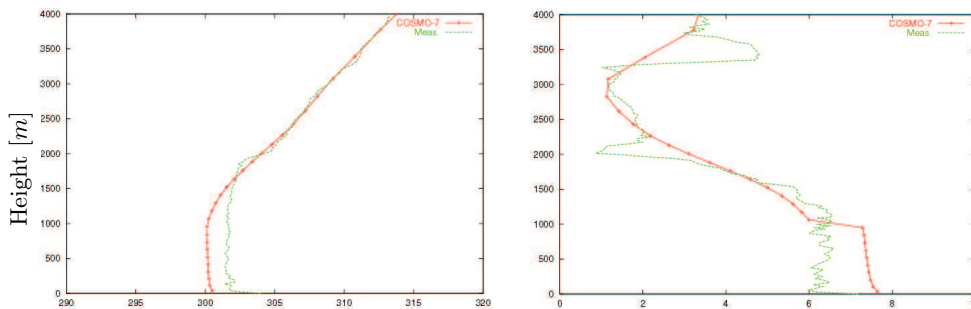


Figure 4: Forecasted vertical profiles of the COSMO-7 model (red line) compared to the radiosounding (green line) at Lindenberg on 18 July 2006 at 12 UTC. Left panel: virtual potential temperature [K]; right panel: specific humidity [g/kg].

Table 2: Number of cases during stable days, when the different methods were able to diagnose a PBL height (maximum number was 93).

<b>Ri</b> <b>(0.38)</b>	<b>TKE</b> <b>(0.2)</b>	<b>Mom. Fl.</b> <b>(0.2)</b>	<b>Heat Fl.</b> <b>(0.2)</b>	<b>Zil.</b>	<b>Bulk Ri</b> <b>(0.33)</b>
32	65	82	75	93	54

was not the case for stable situations. A method was considered unsuccessful in this respect, if either the diagnosed PBL top was at the first model level (i.e. 30 m by COSMO-7 and 10 m by COSMO-2), or no PBL top was found below 5000 m. The first case was mainly associated with the Richardson number methods, while the second case with methods based on TKE or the turbulent fluxes. The number of successful diagnoses (Table 2) was the highest with the momentum flux method and lowest with the gradient Richardson number method. The diagnostic method based on the Zilitinkevich equation could give a PBL height in every case as the only condition to solve this equation is that the surface heat flux should be negative.

To be able to perform a fair intercomparison between the different methods, verification scores were calculated only for those cases when all the methods were successful in finding a PBL top. These verification scores for COSMO-7 forecasts during stable days are shown in Table 3. The biases of the different approaches do not show such a clear tendency as the definitive underestimation observed during convective situations. For stable days the Zilitinkevich method shows the smallest biases with a slight underestimation. Also an underestimation could be observed when using momentum fluxes or the gradient Richardson number. However, in the case of TKE, heat flux and the bulk Richardson number method, a clear overestimation is shown, which corresponds to the above mentioned assumption of the too active stable boundary layer in the model. Concerning the root mean square error, the method based on the Zilitinkevich equation performs best followed by the bulk Richardson number method and the momentum flux approach

Finally, it has to be noted, that using radiosoundings to determine the height of the stable boundary layer is rather difficult and consequently the verification results should be handled with certain caution. The subjective evaluation of the radiosounding profiles showed that the above mentioned automatic methods could provide too high values during stable conditions.

Table 3: Verification scores for stable cases.

	<b>Ri</b> <b>(0.38)</b>	<b>TKE</b> <b>(0.2)</b>	<b>Mom. Fl.</b> <b>(0.2)</b>	<b>Heat Fl.</b> <b>(0.2)</b>	<b>Zil.</b>	<b>Bulk Ri</b> <b>(0.33)</b>
<b>BIAS (m)</b>	-230.1	814.9	-146.7	240.8	-114.6	-12.9
<b>BIAS-rel</b>	-0.425	3.1	-0.148	1.193	-0.095	0.14
<b>STDEV (m)</b>	191.3	603.4	189.1	391.9	181	176
<b>RMSE (m)</b>	246.2	839	191.4	344.2	164.7	133.1
<b>RMSE-rel</b>	0.572	3.14	0.448	1.328	0.404	0.424

## 4 Summary and Outlook

Different turbulence coupling approaches between the COSMO model and the Lagrangian Particle Dispersion Model have been investigated. It has been shown that the TKE in the dispersion model is highly sensitive to the chosen coupling type. Occasional unrealistic oscillations in the COSMO model – which are considered to be a result of numerical instability – could also have an impact on the post-diagnosis of the turbulence fields.

To be able to compare the turbulence characteristics of the COSMO model with scaling considerations, different methods for diagnosing the boundary layer height from COSMO outputs have been tested and validated against radiosounding data. Next to the theoretical approaches, the momentum fluxes of the COSMO model proved to be a good indicator of the PBL height.

As a next step, PBL heights from the COSMO model are planned to be verified against LIDAR measurements, which are considered to be more reliable than radiosoundings in stable conditions. An extensive testing of the COSMO models turbulence scheme is also planned in the framework of the COSMO Priority Project UTCS. The turbulence characteristics of the COSMO model are going to be compared with measurements and LES data, to achieve a better understanding of the model's performance.

## References

- Batchvarova, E. and S.E. Gryning, 1991: Applied model for the growth of the daytime mixed layer. *Boundary-Layer Meteorol.*, 56, 261-274.
- Doms, G. and U. Schättler, 2002: The nonhydrostatic limited-area model LM - Part I: Dynamics and Numerics. Deutscher Wetterdienst, Offenbach, Germany (available from <http://www.cosmo-model.org>).
- Glaab, H., B. Fay B. and I. Jacobsen, 1998: Evaluation of the emergency dispersion model at the Deutscher Wetterdienst using ETEX data. *Atmos. Environ.*, 32, 4359-4366.
- Mellor, G.L. and T. Yamada, 1982: Development of a turbulence closure model for geophysical flow problems. *Rev. Geophys. and Space Phys.*, 20, 851-875.
- Vogelzang, D.H.P. and A.A.M. Holtslag, 1996: Evolution and model impacts of alternative boundary layer formulations. *Boundary-Layer Meteorol.*, 81, 245-269.
- Wetzel, P.J., 1982: Toward parametrization of the stable boundary layer. *J. Appl. Meteorol.*, 21, 7-13.
- Zilitinkevich, S., I. Esau and A. Baklanov, 2007: Further comments on the equilibrium height of neutral and stable planetary boundary layers. *Q. J. R. Meteorol. Soc.*, 133, 265-271.

## An Advanced Snow Parameterization for Models of Atmospheric Circulation

EKATERINA E. MACHUL'SKAYA<sup>1,2</sup>, VASILY N. LYKOSOV<sup>1,3</sup>

<sup>1</sup>*Institute for Numerical Mathematics, Russian Academy of Sciences, Moscow, Russia*

<sup>2</sup>*Hydrometeorological Centre of Russian Federation, Moscow, Russia*

<sup>3</sup>*Moscow State University, Russia*

### 1 Introduction

Numerous observational studies and climate model simulations have shown that snow cover affects atmospheric circulation, air temperature, and the hydrologic cycle. Snow cover, especially fresh snow, has a much higher albedo than bare ground or liquid water, so that solar radiation absorption is significantly reduced, often as much as 50%. The induced radiative cooling is reinforced by the high thermal emissivity of the snow cover, which increases static stability in the atmospheric boundary layer and consequently reduces turbulent fluxes. This effect is enhanced by a reduced roughness of snow-covered vegetation when compared to snow free conditions.

Snow extent is related to a number of feedbacks, the most obvious being the snow albedo feedback: a positive temperature bias (for instance, as a result of a global climate change) leads to larger snow melt, faster snow cover depletion, which leads to a decrease of surface albedo. This allows more absorption of solar radiation and therefore reinforces further warming.

To represent land surface processes in atmospheric models different schemes have been developed, including soil-vegetation-atmosphere transfer schemes that incorporate snow models of the different complexity (e.g. Sellers et al., 1996, Bonan, 1996, Verseghy, 1991, Desborough and Pitman, 1998, Gusev and Nasonova, 1998, Volodin and Lykosov, 1998, Volodina et al., 2000).

At the moment many time series of different meteorological and hydrological characteristics have been accumulated from different field experiments and regular observations. It makes possible thorough evaluation and intercomparison of snow models to understand what snow processes must be represented in the coupled land surface schemes and atmospheric models.

The present study reports results of comparative analysis of the snow depth simulation obtained with two land surface schemes, namely the land surface scheme TERRA of the COSMO model (Doms et al., 2005) and one (Volodina et al., 2000) of the global circulation model of the Institute for Numerical Mathematics (INM) (Moscow, Russia). This intercomparison is done by means of the meteorological and hydrological data sets that were continuously collected at Valdai water-balance research station (Russia, European part) in 1966–1983 and at Yakutsk meteorological research station (Russia, East Siberia) in 1937–1984.

### 2 Brief description of models

The land surface scheme of the COSMO model has 7 layers in the soil (the depth of the 7th layer is 4.86 m, and there is one additional climatological layer at the depth of 14.58

m) and one layer to describe the snowpack properties, namely snow temperature, snow water equivalent depth and snow density. The temperature profile in the soil is predicted by the heat conduction equation and then adjusted against liquid/frozen water content (freezing/melting), and the snow temperature is calculated following the heat conduction and energy budget at the snow surface. When snow temperature rises upon the melting point, it is set to the melting point value and the excess of the heat is spent to melt the snow. This amount of the melted water immediately appears on the soil surface, and snow water equivalent depth decreases. Snow density varies accordingly to an empirical formula that accounts for the snow age, i.e., the old snow density is greater than the fresh snow density. It is taken that the fresh snow has a density of  $250 \text{ kg/m}^3$ .

In the land surface scheme of the INM model, it is possible to use an arbitrary number of soil layers (in the current study it was fixed at 32), the lowest layer locates at the depth of 10 m. In the snow model, constructed on the basis of studies on snow dynamics (e.g., Bengtsson, 1982; Colbeck, 1978; Glendinning and Morris, 1999; Pomeroy et al., 1998), an arbitrary number of layers in the snowpack is also used (in this study, 5 layers). The temperature profile in the soil and in the snow is also computed by the heat conduction equation and then adjusted against liquid/frozen water content. This adjustment is carried out not only in the soil, but also in the snow: any layer of the snowpack can contain the liquid water up to water holding capacity. This liquid water can refreeze, if the layer temperature falls under the freezing point. When the liquid water content of the layer becomes greater than water holding capacity of the snow, this water percolates into underlying layer. Snowmelt starts, i.e., snow water equivalent depth decreases, only when liquid water content of the lowest snow layer is greater than water holding capacity, and water from this layer percolates to the soil surface.

Besides the water refreezing and percolation processes, in the INM snow model the other processes are implemented — gravitational compaction and metamorphosis of the snow (Marshall et al., 1999) and the solar radiation penetration through the snowpack (Jordan, 1991). The density of each snow layer is analytically calculated accordingly to content of snow, liquid and frozen water in the layer. The fresh snow density depends on the air temperature and can vary from 65 to  $145 \text{ kg/m}^3$  (Hedstrom and Pomeroy, 1998). Further, to describe effects of the gravitational compaction of snow, a semi-empirical formula (Marshall et al., 1999) is employed.

After implementing all of these physical processes into the INM snow model, the computational cost increased of 7 per cent, when compared with the first version of this model that was similar to the present COSMO snow model.

### 3 Data

Two observational data sets were used for numerical experiments. The first data set contains long-term systematical observations that were collected in 1966–1983 at a grassland site at the Valdai water-balance research station (57.6N, 33.1E) in the forest zone of Russia. This data has been used as forcing and evaluation data for the land surface simulations during the frame of the Project for Intercomparison of Land-surface Parameterization Schemes (PILPS), Phase 2(d) experiment. The forcing data with 3-hour temporal resolution contains measurements of the downward shortwave and longwave radiation, precipitation rate, air temperature, pressure and specific humidity at the 2 meter height and horizontal components of the wind speed at the 10 meter height. The evaluation data contains, among other parameters, time series of the snow water-equivalent depth that were measured every 10 days in winter and more often in spring.

The second data set is similar to the first one, but was collected at the Yakutsk meteorological station (East Siberia) in 1937–1984. Due to the lack of observations of the solar radiation at this station, to estimate the incoming shortwave and longwave radiation, some empirical formulae, containing information on the cloudiness, air temperature, humidity and pressure, station’s latitude and longitude, were used.

#### 4 Results and discussion

In general, both models reasonably represent the water-equivalent snow depth (SWE) and the onset of intensive snow melting.

For Yakutsk, the models under consideration have shown close results. The moment of complete disappearance of the snow cover is represented very close to observations, but the simulated SWE is systematically overestimated by both models during the late winter and spring. SWE, simulated by the INM model, is a little bit more close to the observed SWE than SWE, simulated by the TERRA (Fig. 1).

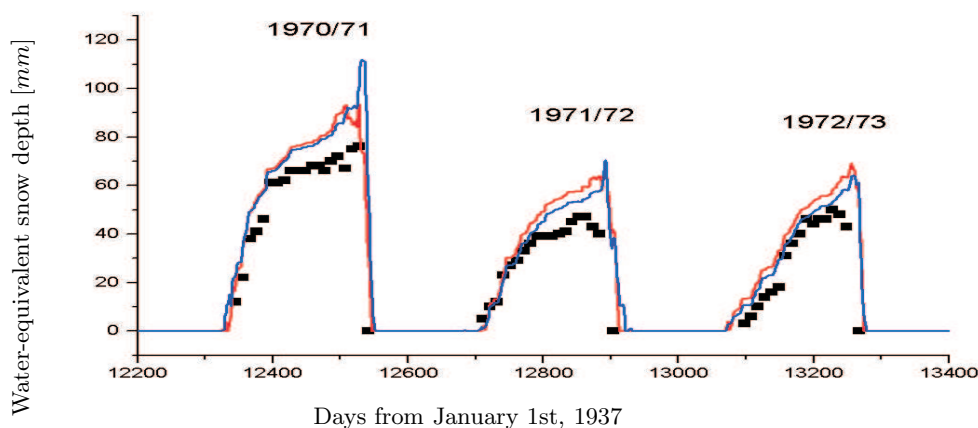


Fig. 1: Observed (black symbols) and simulated by TERRA and INM models (red and blue lines, respectively) water-equivalent snow depth, Yakutsk.

For Valdai, there are more differences in results of modeling. In the TERRA model, snow melts much earlier than in the INM model and than in reality. As summarized in Table 1, the correlation coefficient between time series of observed and simulated by TERRA and INM models snow water equivalent depth is 0.71 and 0.90, respectively. Mean errors in the time of the snow complete ablation are -17 (7) days in the TERRA model versus -1 (1) day in the INM model.

Table 1: (a) The correlation coefficient ( $r$ ) between time series of observed and simulated by the TERRA and INM models snow water equivalent depth and (b) mean error ME ( $\pm$  standard deviation SD) in the time of the snow complete ablation at the Valdai station.

	(a) $r$	(b) ME $\pm$ SD, days
TERRA	0.71	-17 ( $\pm$ 7)
INM	0.90	-1 ( $\pm$ 1)

In Fig. 2, time series of SWE, observed and simulated by both models for the 9 first years starting from 1967, are shown. It should be noted that within this study the first year of

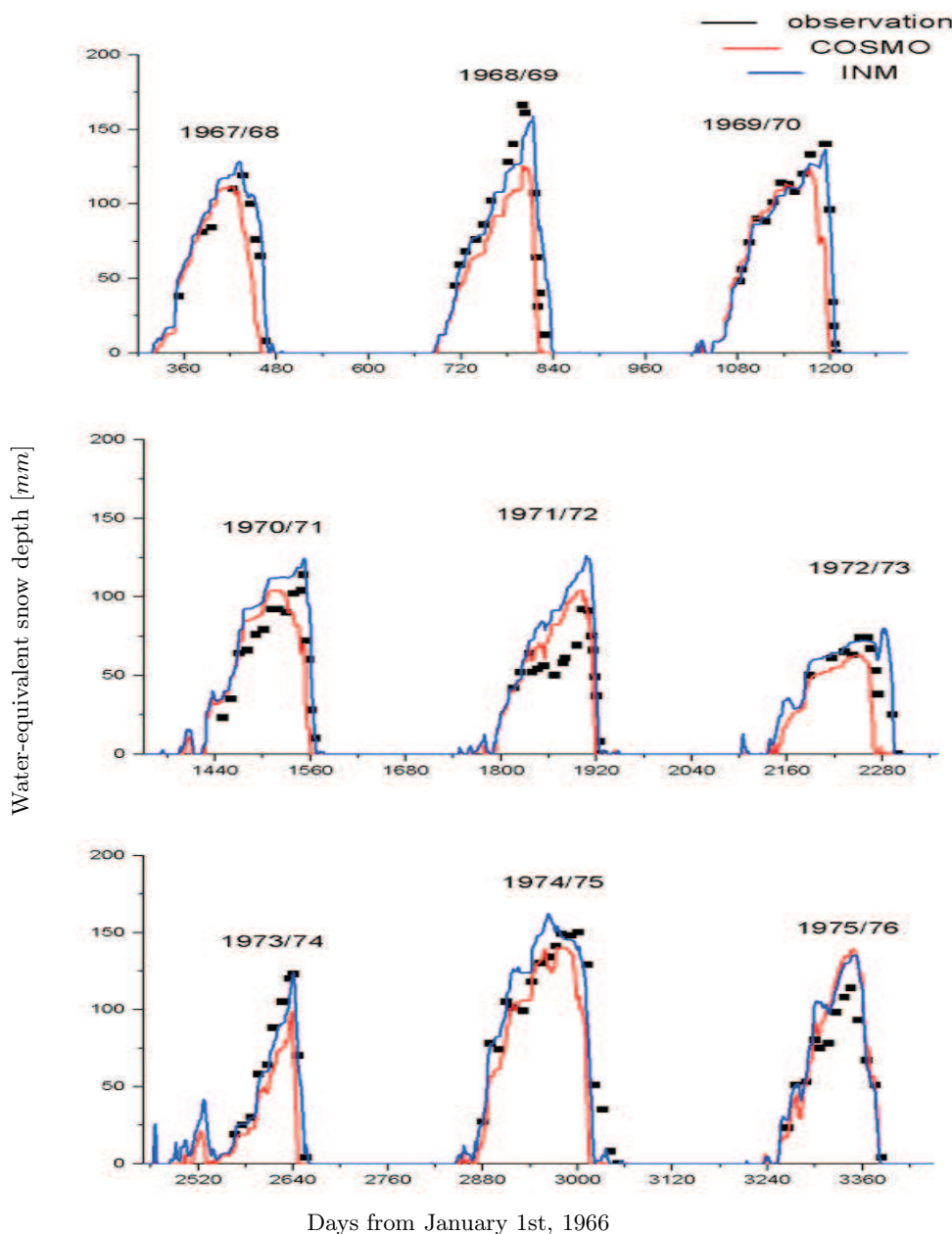


Fig. 2: Observed (black symbols) and simulated by TERRA and INM models (red and blue lines, respectively) snow water-equivalent depth, Valdai, 1967-1976.

integration, 1966, is considered as a spin-up period and is not included into analysis of the results. For the last 8 years, the pattern of difference between observed and simulated SWE is the same. The discrepancy between results of snow depth simulation by TERRA and INM models is more noticeably in the late winter and particularly during the spring.

This discrepancy can be explained by difference in the models descriptions of physical processes in snow. It is known that there is a delay between the onset of snowmelt at the snow surface and decrease of the SWE. Before the melted water can leave a snowpack, the cold content, i.e., negative heat stored in snow, must be overcome, and the snow saturation must be increased to its irreducible liquid saturation. The percolation rate of melted water depends on the hydraulic conductivity of the snow, but also very strongly on the degree of saturation of the snow. Even when the entire snowpack is at the freezing point and is saturated to its

irreducible liquid content, the first amount of the melted water may need many hours to percolate from the snow surface to the snowpack base. Hence a snowpack can undergo many repeated cycles of the day-time snowmelt and night-time refreezing of liquid water, before any melted water leaves the snowpack.

It should be noted that the adequate prediction of the melting rate of the snow and time of its complete ablation is of particular importance for the weather forecasting since these processes determine the moment, after which the ground temperature starts to rise above the freezing point value. This, in turn, affects the air temperature, too. Figure 3 shows how surface temperatures are affected by snow melting process on the time scale of several days before and after snow ablation. Unfortunately surface temperature measurements with sufficient time resolution are not available (monthly mean values only), so we just have a possibility to intercompare the surface temperature evolution simulated by the models under consideration. One can see that during 10 - 20 days when snow in TERRA is completely melted and in INM it is not, there is a noticeably difference between daily mean values of the surface temperature.

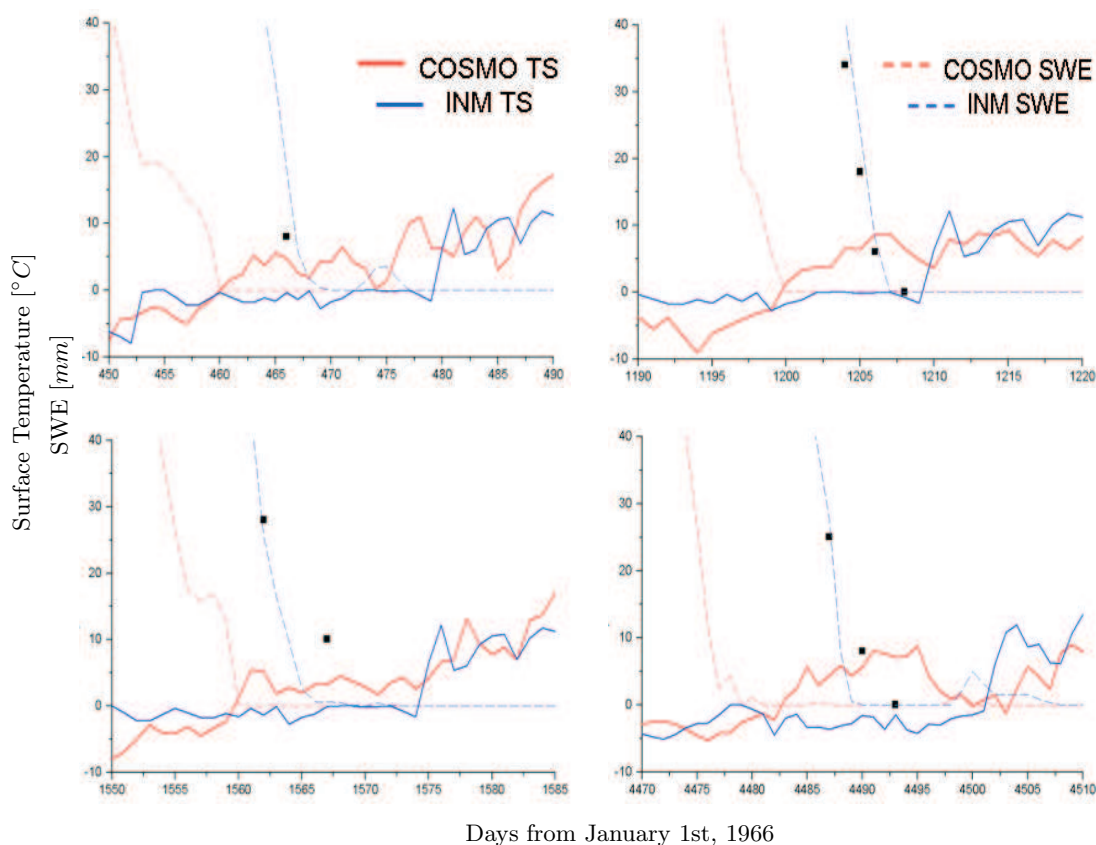


Fig. 3: Observed (black symbols) SWE and simulated by TERRA and INM models (red and blue lines, respectively) SWE (dashed lines) and surface temperature (solid lines), for 4 different years at Valdai.

In Yakutsk, in comparison with Valdai, the snow ablation is more rapid, at least, in those years when the snow depth observational data is available. The period of intensive melting lasted in these years a few days. Probably, this is the cause why in Yakutsk the aforementioned differences in the models results do not appear. In Valdai, the spring snow temperature many times passes through the freezing/melting point and that is why liquid water content

noticeably influences the results. It should be noted that Valdai is situated in mid-latitudes of European part of Russia and the spring atmospheric conditions of this region are more close to the atmospheric conditions of Europe than to the strongly continental conditions of Yakutsk. Therefore, one can expect that processes related to liquid water in snow could be important for European territory, as well as for Valdai.

Together with the liquid water percolation and refreezing, the gravitational compaction and penetration of the solar radiation (which are also parameterized in the INM snow model) can affect the snow depth and the melting rate, too. An analysis has shown that processes of the snow metamorphosis and compaction due to gravity have a little impact on SWE in Valdai. Processes of the shortwave radiation penetration essentially delay the snow ablation. When the solar radiation, incoming onto the snow surface, does not penetrate into the snowpack, the whole amount of solar energy is spent to melt the top snow layer. In the case of penetrating radiation, the amount of incoming energy is distributed between some layers, and specific amount of energy is lesser in this case.

It is very useful to use a long-term continuous observational data, because during numerical experiment a great number of different meteorological conditions and situations can occur. Thus it is possible to determine the contribution of different physical processes to the modeling results and to understand the relative importance of each of them.

## 5 Summary and Outlook

In conclusion, some recommendations for the further development of the COSMO snow model, derived from results of the above presented analysis, can be suggested. Namely, the implementation of new parameterizations of the snow processes, particularly, taking into account transport of the snow liquid water and penetration of the solar radiation, can improve quality of simulation of the snow water equivalent depth.

It should be noted also that the Valdai observational data set includes data related to the snow density and albedo, as well as to the snow cover fraction. It is known that fractional snow cover, snow albedo, and their interplay have a considerable effect on the energy available for ablation (Slater et al., 2001; Luce et al., 1998). The scale of these processes (10–100 m) is much smaller than the grid resolution of most LSMs (10–100 km) (Pomeroy et al. (2003)). In both COSMO and INM models, the snow albedo is obtained from empirical formulae, and snow cover fraction linearly depends on SWE, when SWE is lesser than some critical value. Thus, the observational albedo and snow cover fraction data allows to further evaluate the COSMO snow model and to understand to what extent the adequate simulation of these variables is important, in order to improve the prediction of processes of the snow accumulation and ablation.

This study was financially supported by the Russian Foundation for Basic Research (grants 07-05-00200 and 07-05-13566).

## References

- Bonan, G. B., 1996: A Land Surface Model (LSM version 1.0) for Ecological, Hydrological, and Atmospheric Studies: Technical Description and Users Guide, *NCAR Tech. Note NCAR/TN-417+STR*, 150 pages.
- Colbeck S. C., 1978: The Physical Aspects of Water Flow through Snow, *Adv. Hydrosoci.*, V.11, 165–206.
- Desborough, C. E., and A. J. Pitman, 1998: The BASE Land Surface Model, *Global Planet.*

*Change*, 19, 3–18.

Doms G., J. Förstner, E. Heise., H.-J. Herzog, M. Raschendorfer, R. Schrodin, T. Reinhardt, G. Vogel, 2005: A Description of the Nonhydrostatic Regional Model LM. Part II: Physical Parameterizations, *Deutscher Wetterdienst*, Offenbach, 139 pages. Available at: [www.cosmo-model.org](http://www.cosmo-model.org).

Glendinning J.H.G., and E. M. Morris, 1999: Incorporation of spectral and directional radiative transfer in a snow model. *Hydrol. Process.*, 13, 1761–1772.

Gusev Ye. M., and O. N. Nasonova, 1998: The land surface parameterization scheme SWAP: description and partial validation. *Global and Planetary Change*, V. 19, p. 63–86.

Hedstrom, N., and J. W. Pomeroy, 1998: Intercepted snow in the boreal forest: measurement and modeling, *Hydrol. Process.*, 12, 1611–1625.

Jordan R., 1991: A one-dimensional temperature model for a snow cover. *Technical documentation for SNTHERM.89*, US Army Corps of Engineers, CRREL Special Report 91–16.

Luce, C. H., D. G. Tarboton and K. R. Cooley, 1998: The influence of the spatial distribution of snow on basin-averaged snowmelt, *Hydrological Processes*.

Marshall, H. P., H. Conway, and L. A. Rasmussen, 1999; Snow densification during rain, *Cold Reg. Sci. and Tech.*, V.30, pp. 35–41.

Pomeroy, J. W., D. M. Gray, K. R. Shook, B. Toth, R.L.H. Essery, A. Pietroniro, N. Hedstrom, 1998: An evaluation of snow accumulation and ablation processes for land surface modeling. *Hydrol. Process.*, 12, 2339–2367.

Schlosser, C. A., A. Robock, K. Ya. Vinnikov, N. A. Speranskaya, and Y. Xue, 1996: 18-year land-surface hydrology model simulations for a midlatitude grassland catchment in Valdai, Russia, *Mon. Wea. Rev.*, 125, 3279–3296.

Sellers, P. J. and Coauthors, 1996: A revised land surface parameterization (SiB2) for atmospheric GCMs. Part I: Model formulation. *J. Climate*, 9, 676–705.

Slater, A.G., C. A. Schlosser, C. E. Desborough, A. J. Pitman, A. Henderson-Sellers, A. Robock, K. Y. Vinnikov, K. Mitchell, A. Boone, H. Braden, F. Chen, P. M. Cox, P. de-Rosnay, R. E. Dickinson, Y. J. Dai, Q. Duan, J. Entin, P. Etchevers, N. Gedney, Y. M. Gusev, F. Habets, J. Kim, V. Koren, E. A. Kowalczyk, O. N. Nasonova, J. Noilhan, S. Schaake, A. B. Shmakin, T. G. Smirnova, D. Verseghy, P. Wetzal, X. Yue, Z. L. Yang, and Q. Zeng, 2001: The representation of snow in land surface schemes: results from PILPS-2d. *J. Hydrometeorol.*, 2, 7–25.

Verseghy, D., N. McFarlane and M. Lazare, 1991: CLASS — A Canadian Land Surface Scheme for GCMs. I. Soil model. *Int. J. Climatol.*, 13, 111–133.

Volodin, E.M., V. N. Lykosov, 1998: Parameterisation of heat and moisture transfer in the soil-vegetation system for use in atmospheric general circulation models. 1: Formulation and simulations based on local observational data. *Izvestiya. Atmospheric and Oceanic Physics*, V. 34, pp. 453–465.

Volodina E. E., L. Bengtsson, V. N. Lykosov, 2000: Parameterization of heat and moisture transfer through snow pack for simulation of seasonal variations of land-surface hydrologic cycle. *Russian Journal of Meteorology and Hydrology*, No. 5, pp. 5–14.

## Revision of the Turbulent Gust Diagnostics in the COSMO Model

JAN-PETER SCHULZ

*Deutscher Wetterdienst, Offenbach a. M., Germany*

### 1 Introduction

Verification has shown that the gusts in analyses and forecasts of the COSMO-EU model are systematically overestimated (e.g. Göber 2007). This is most obvious in storm systems during the winter season. COSMO-EU, formerly known as LME (see e.g. Schulz 2006), is an operational implementation of the COSMO model (Doms and Schättler 2002) at the German Weather Service (DWD), covering almost all Europe using a mesh size of 7 km.

The gust formulation of COSMO consists of two components: turbulent gusts and convective gusts (Schulz and Heise 2003). An analysis has shown that the turbulent gusts are responsible for the overestimation in the cases considered here. A revised formulation of the turbulent gust diagnostics is presented here which considerably reduces the bias in a number of case studies as well as in a numerical experiment with a length of a few weeks.

### 2 Diagnosing near-surface turbulent gusts

In the COSMO model the maximum turbulent gusts at 10 m above the ground are derived from the turbulence state in the atmospheric boundary layer, using the absolute speed of the near-surface mean wind  $V_m$  and its standard deviation  $\sigma$ :

$$V_{\text{turb}} = V_m + \alpha \sigma \quad (1)$$

$$V_{\text{turb}} = V_m + \alpha 2.4 u_* \quad (2)$$

$$V_{\text{turb}} = V_m + \alpha 2.4 \sqrt{C_D} V_m \quad (3)$$

The step from (1) to (2) uses an empirical relation between  $\sigma$  and the friction velocity  $u_*$ . The value 2.4 is given for instance in Panofsky and Dutton (1984), it is a mean empirical value derived from several observation campaigns.  $C_D$  is the drag coefficient for momentum. The parameter  $\alpha$  has been estimated to  $\alpha = 3$ .

In the original version of the COSMO model (Doms and Schättler 2002) as of 1999 (35 levels, lowest one about 30 m above the ground) the absolute mean wind speed at the lowest level was taken for  $V_m$  in (3). When introducing the 40 vertical levels (Schulz 2006) in 2005 (lowest one about 10 m above the ground) the formulation was adapted, in order to keep the tuning, by interpolating  $V_m$  at 30 m from the two lowest model levels (while computing the friction velocity by definition from the speed at the lowest model level). The same procedure had been done in the global model GME before when changing to the 40 level version, and it was repeated here in order to stay consistent with the driving model. But this formulation leads to the overestimation of the gusts in COSMO-EU.

In the revised version presented here the wind speed at 10 m above the ground is taken for  $V_m$ , while an effort was made to keep this 10-m wind independent of the vertical discretisation.  $\alpha$  is kept at a value of 3.

### 3 Case studies

Six storm cases in the first half of 2007 were identified from the reports of the DWD department issuing the weather warnings. In all cases COSMO-EU has overestimated the gusts. They have all been tested with the revised version of the model, four cases are presented here.

When testing the gust diagnostics the problem arises that the COSMO model also shows a tendency to overestimate the intensity of low pressure systems in terms of core pressure and pressure gradient. This could already explain the overestimation of the gusts. In order to exclude this additional uncertainty only cases are considered where the simulated pressure field is very close to the observed one, which is usually the case for the analyses and the very first forecast hours. It turned out that in all six cases the overestimation of the gusts already appears in the first forecast hour.

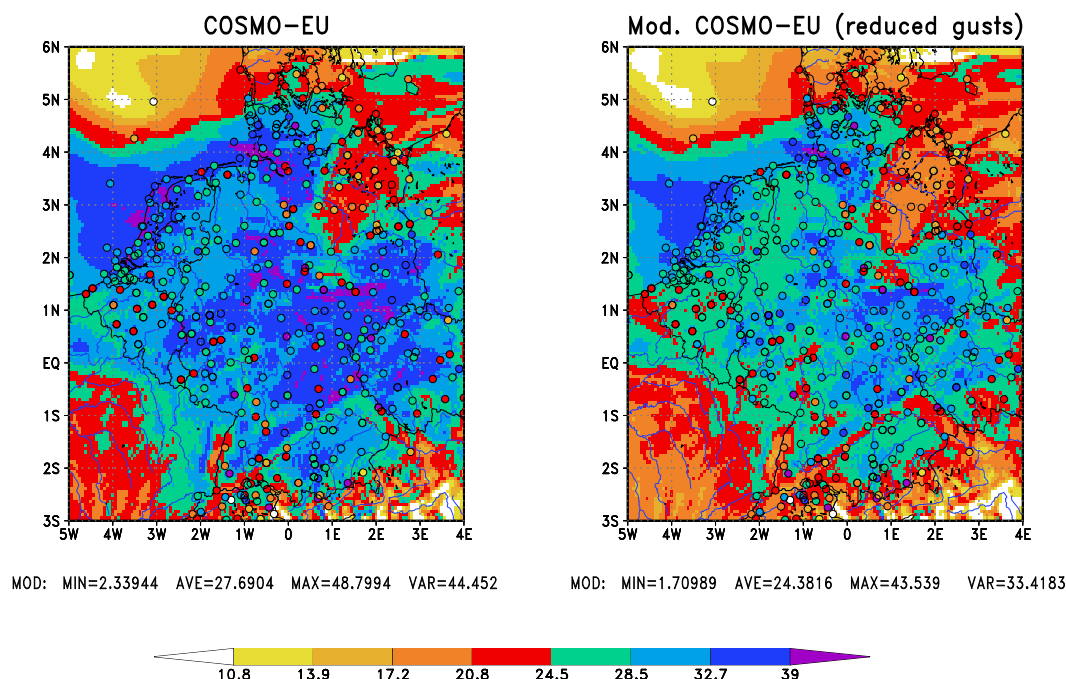


Figure 1: Comparison of 10-m gusts (m/s) on 18 Jan. 2007, 18 UTC + 01h, as forecasted by the operational COSMO-EU and by the modified COSMO-EU using the revised diagnostics for turbulent gusts. The circles in the maps are observations.

The first case presented here occurred on 18 Jan. 2007. It got the name “Kyrill” and received probably the highest attention in German media of all storms during this winter season due to its wind speeds, the spatial extent and the destructions it caused. Figure 1 shows the 10-m gusts from the operational forecast of COSMO-EU and compares them to the gusts predicted by the revised model version. The forecasts on 18 Jan. 2007 at 18 UTC + 01h were selected, this was the time when the gusts reached their peak values in some parts of southern and western Germany. The reference period for the maximum gusts which are reported at this hour is the preceding hour, this means the period 18–19 UTC. The operational forecast shows wide areas in Germany and the surrounding countries with gusts of 12 Bft (dark blue and purple) or 11 Bft (blue). In the revised model version these gusts are reduced by about 1 Bft, turning dark blue areas into blue, and blue areas into green. In the other speed intervals we find a similar behaviour.

The overestimation of the gusts in the operational forecast becomes very obvious when comparing it to the observations, indicated by coloured circles in the maps. All available

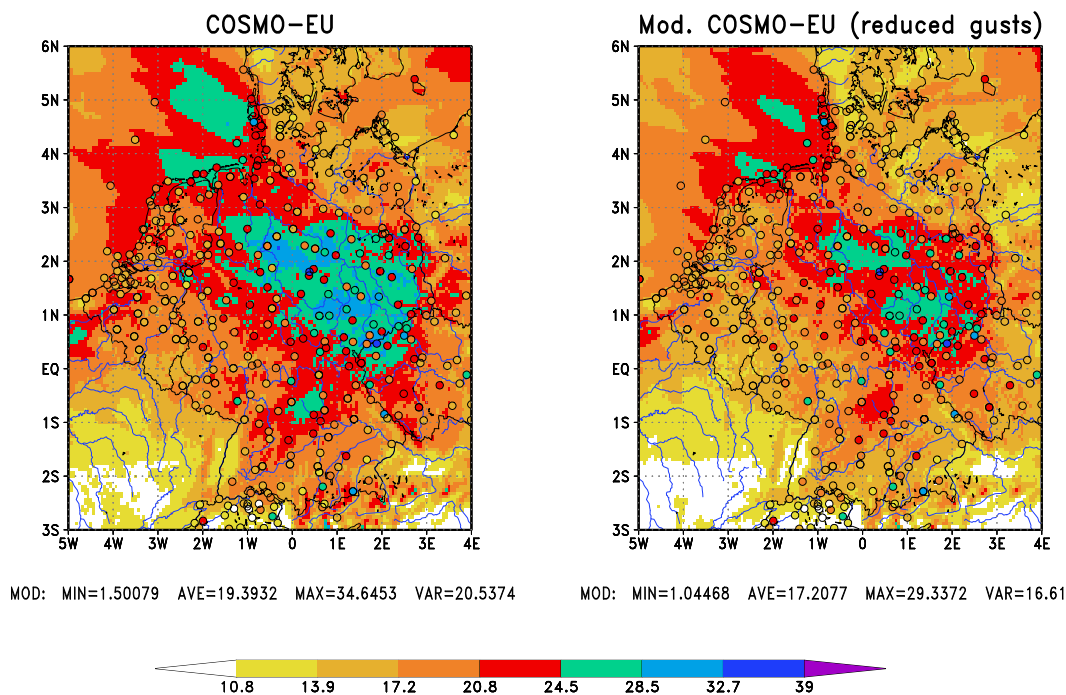


Figure 2: Comparison of 10-m gusts (m/s) on 21 Jan. 2007, 12 UTC + 01h, as forecasted by the operational COSMO-EU and by the modified COSMO-EU using the revised diagnostics for turbulent gusts. The circles in the maps are observations.

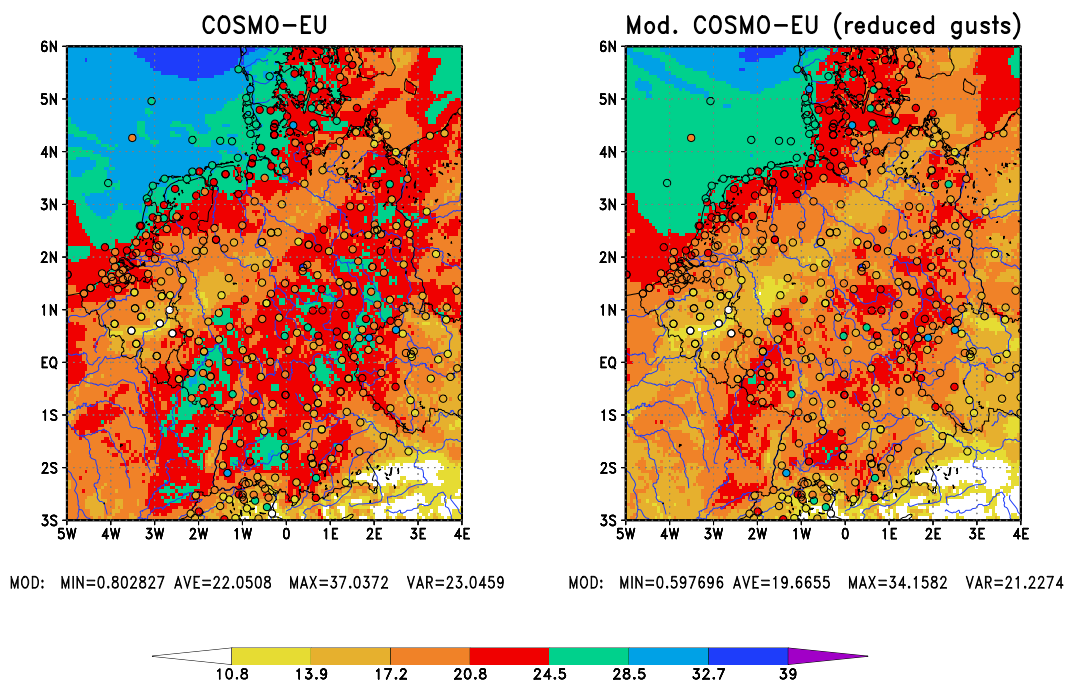


Figure 3: Comparison of 10-m gusts (m/s) on 18 Mar. 2007, 12 UTC + 01h, as forecasted by the operational COSMO-EU and by the modified COSMO-EU using the revised diagnostics for turbulent gusts. The circles in the maps are observations.

SYNOP observations were used here. The overestimation reaches from 1 Bft (e.g. green circles on blue shading) up to 3 Bft (red circles on dark blue shading). In the revised model version the gusts are reduced which leads to a considerable improvement, model and observations match much better at most places.

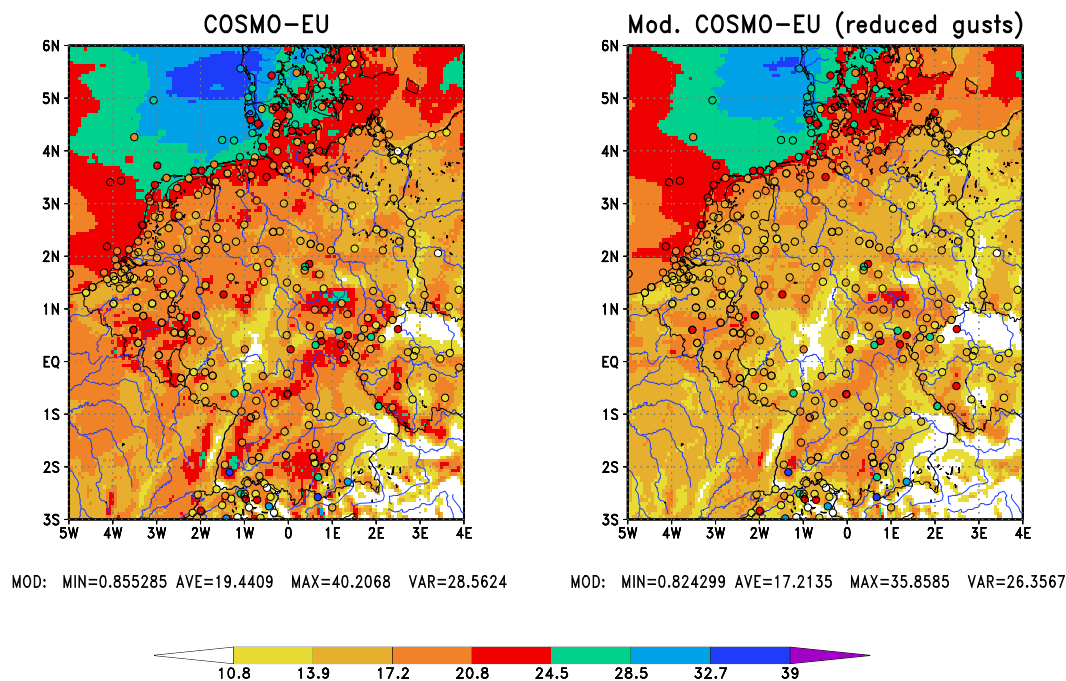


Figure 4: Comparison of 10-m gusts (m/s) on 01 Jan. 2007, 06 UTC + 01h, as forecasted by the operational COSMO-EU and by the modified COSMO-EU using the revised diagnostics for turbulent gusts. The circles in the maps are observations.

The three other cases (Figs. 2-4) show generally a similar behaviour. The operational forecasts were overestimating the gusts, although less pronounced than for the Kyrill case, while the reduced gusts of the revised model are in better agreement with the observations at most places. There are a few stations in mountainous areas which report much higher gust values than forecasted by both model versions. The reason is that these observations do most likely not fulfill the standards for measuring 10-m gusts, which would mean that they were representative for an undisturbed area of at least a few squarekilometers, providing an open flat terrain causing only minor alterations due to topographic effects. If this not the case it can not be expected that the COSMO-EU gusts which are computed on a  $7 \text{ km} \times 7 \text{ km}$  grid are comparable to this kind of observations.

#### 4 Numerical parallel experiment

Besides the case studies the new formulation was also tested in a continuous numerical parallel experiment, repeating the operational forecasts. The period was 10 – 25 Jan. 2007. Figure 5 shows the observed mean gusts and also the observed ratio of mean gusts divided by mean wind speed, both versus mean wind speed. In this figure all available reports from 192 sites in Germany at heights between 0 and 500 m were used. Furthermore, the figure shows a systematic overestimation of the gusts by the operational COSMO-EU, as known from the case studies. On the other hand, the revised model version is almost free of bias.

There seems to be a little drawback for the high gusts which appear to be slightly underestimated in the revised model version. This behaviour seems to be caused by a few mountainous stations as discussed in the section before. Returning to the argument of representativeness, gust reports from airports would be expected to be of highest quality and most representative for an undisturbed area of at least a few squarekilometers and therefore best to be compared to a mesoscale model. This is done in Fig. 6 which shows the same as Fig. 5,

but only for observations at 17 German airports. With regard to these observations also the revised diagnostics still slightly overestimates the gusts. This is favourable in terms of the warning process which usually prefers a slight overwarning by the model.

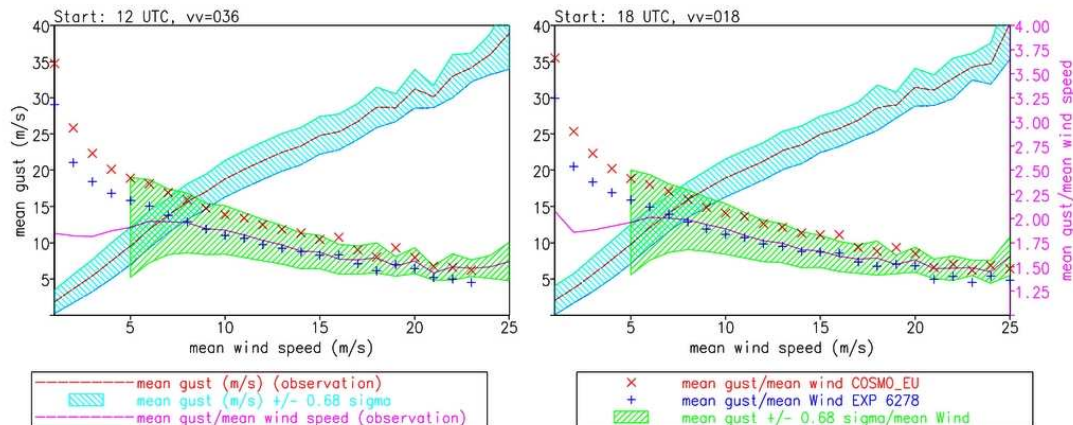


Figure 5: Observed mean gusts versus mean wind speed (blue shading, scale at left ordinate), observed ratio of mean gusts divided by mean wind speed, also versus mean wind speed (green shading, scale at right ordinate), both for the period 10 – 25 Jan. 2007. All available reports from 192 sites in Germany at heights between 0 and 500 m were used here. The red x-signs indicate the ratio of mean gusts divided by mean wind speed in the forecasts of the operational COSMO-EU, showing a systematic overestimation of the gusts. The blue plus-signs show the same ratio but for the COSMO-EU version with revised turbulent gust diagnostics. The latter is almost free of bias. This figure was provided by U. Damrath, DWD.

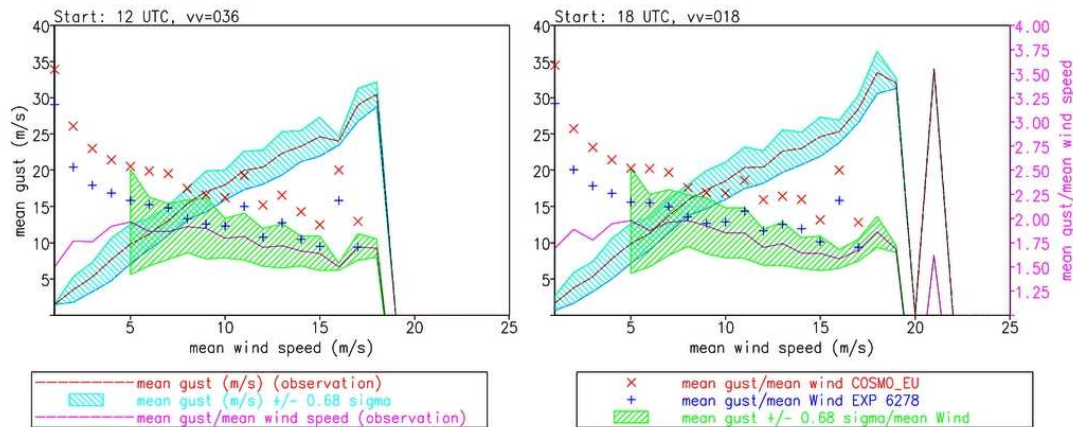


Figure 6: Same as Fig. 5, but only for observations at 17 German airports (below 500 m). With regard to these observations also the revised diagnostics still slightly overestimates the gusts, which is favourable in terms of the warning process. This figure was provided by U. Damrath, DWD.

## 5 Conclusions

Six storm cases were identified in the first half of 2007 in which COSMO-EU has overestimated the gusts. In two cases the overestimation is low (up to 1 Bft), in the four other cases it is higher (up to 2-3 Bft). In all cases the overestimation of the gusts already appears in the very first forecast hours when the pressure field is still in very good agreement with the

analysis. Hence, the overestimation is not simply a consequence of a systematic deviation from the real pressure field which may occur during the course of the forecast.

A revised formulation for diagnosing near-surface turbulent gusts for use in the COSMO model has been presented. It has been successfully tested with the selected six cases. The verification of a continuous numerical experiment of a few weeks length shows a good improvement as well.

## References

- Doms, G. and U. Schättler, 2002: A description of the nonhydrostatic regional model LM. Part I: Dynamics and Numerics. *Deutscher Wetterdienst*, Offenbach, 134 pp. (Available at: [www.cosmo-model.org](http://www.cosmo-model.org)).
- Göber, M., 2007: Comparing peaches and apples – on the accuracy of weather warning issued by forecasters and the accuracy of the model guidance. Presentation at the 3<sup>rd</sup> International Verification Methods Workshop, 31 Jan. – 2 Feb. 2007, Reading. (Available at: [http://www.ecmwf.int/newsevents/meetings/workshops/2007/jwgv/workshop\\_presentations/-M\\_Goeber.pdf](http://www.ecmwf.int/newsevents/meetings/workshops/2007/jwgv/workshop_presentations/-M_Goeber.pdf))
- Panofsky, H. A. and J. A. Dutton, 1984: *Atmospheric turbulence – models and methods for engineering applications*. Wiley Interscience, New York, 397 pp.
- Schulz, J.-P., 2006: The new Lokal-Modell LME of the German Weather Service. *COSMO Newsletter*, **6**, 210–212. (Available at: [www.cosmo-model.org](http://www.cosmo-model.org)).
- Schulz, J.-P. and E. Heise, 2003: A new scheme for diagnosing near-surface convective gusts. *COSMO Newsletter*, **3**, 221–225. (Available at: [www.cosmo-model.org](http://www.cosmo-model.org)).

## Five Years of Limited-Area Ensemble Activities at ARPA-SIM: The COSMO-LEPS system

ANDREA MONTANI, CHIARA MARSIGLI, TIZIANA PACCAGNELLA

*Hydro-Meteorological Service of Emilia-Romagna, ARPA-SIM, Bologna, Italy*  
corresponding author: [amontani@arpa.emr.it](mailto:amontani@arpa.emr.it)

### 1 Introduction

COSMO-LEPS is the Limited-Area Ensemble Prediction System developed and implemented by ARPA-SIM within COSMO (Consortium for Small-scale MOdelling; the members of the Consortium are Germany, Greece, Italy, Poland, Romania and Switzerland). COSMO-LEPS project aims to generate “short to medium-range” (48–132 hours) probabilistic predictions of severe weather events based on the non-hydrostatic regional COSMO-model, nested on a number of ECMWF EPS members, chosen via a clustering selection technique (Marsigli et al., 2001).

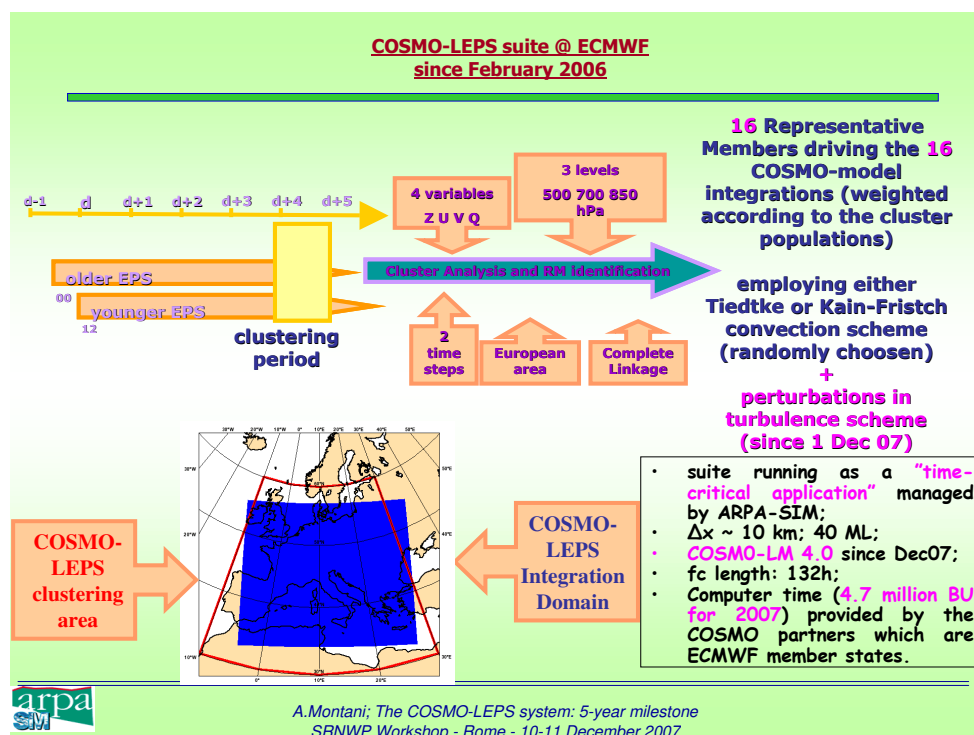


Figure 1: Present set-up of COSMO-LEPS operational suite.

The “experimental-operational” COSMO-LEPS suite (following the methodology described by Montani et al., 2003 and Marsigli et al., 2005) was set up in November 2002 to produce probabilistic forecasts over a domain covering all countries involved in COSMO. After 5 years of activity, COSMO-LEPS application has become an “ECMWF member-state time-critical application” managed by ARPA-SIM and its present configuration is shown in Fig. 1. COSMO-LEPS is made up of 16 members, running at the horizontal resolution of 10 km with 40 model levels in the vertical. The computer-time to run COSMO-LEPS application

on ECMWF supercomputers is provided from allocations to the ECMWF COSMO partners (i.e. Germany, Greece, Italy and Switzerland), whose contributions are joined into a unique “COSMO-account”. Perturbations to the initial and boundary conditions are provided by the different EPS members driving the limited-area integrations. In addition to this, the following model perturbations are introduced:

- perturbations to the convection scheme: within each COSMO–LEPS integration, a random choice between Tiedtke or Kain–Fritsch convection scheme is made;
- perturbations in the maximal turbulent length scale;
- perturbations in the length scale of thermal surface patterns.

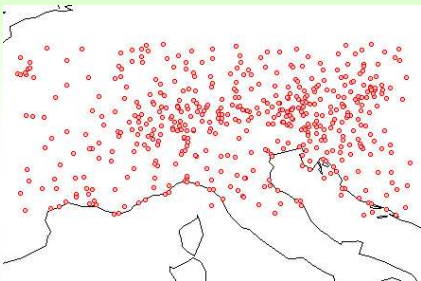
In this contribution, it is assessed the state-of-the-art of the system, showing its ability to provide warnings of severe weather events (e.g. heavy rainfall, strong winds, cold temperature anomalies).

## 2 Results of verification

As already mentioned, COSMO–LEPS has recently passed the 5-year milestone of activity. Therefore, a big verification effort was undertaken so as to assess objectively how the system changed in these years and the extent to which modifications have actually caused an improvement in terms of precipitation forecasts over mountainous areas.

### Objective verification of COSMO-LEPS

- SYNOP on the GTS (COSMO-LEPS only):



**Main features:**

variable: 12h cumulated precip (18-06, 06-18 UTC);

period: **from Dec 2002 to Nov 2007;**

region: 43-50N, 2-18E (**MAP D-PHASE area**);

method: nearest grid point; no-weighted fcst;

obs: synop reports (about 470 stations/day);

fcst ranges: 6-18h, 18-30h, ..., 102-114h, 114-126h;

thresholds: **1, 5, 10, 15, 25, 50 mm/12h;**

system: COSMO-LEPS;

**both (60) monthly and (20) seasonal scores are computed.**

**work is in progress for verification over the full domain (1500 stations)**



A.Montani; The COSMO-LEPS system: 5-year milestone  
SRNWP Workshop - Rome - 10-11 December 2007

Figure 2: Main features of COSMO–LEPS verification.

In order to carry on this evaluation, a fix set of SYNOP stations (about 470) was selected, over an area covering the Alps (43-50N, 2-18E) and for the period ranging from December 2002 to November 2007. Precipitation accumulated over 12 hours (18-06 UTC and 06-18 UTC) was verified, comparing the values forecast on the grid-point nearest to each station against

the observed values at that station. The other main features of the verification exercise are summarised in Fig. 2. Several probabilistic scores were used and the performance of the system was analysed both in terms of monthly and seasonal scores so as to identify the occurrence of possible seasonal variability.

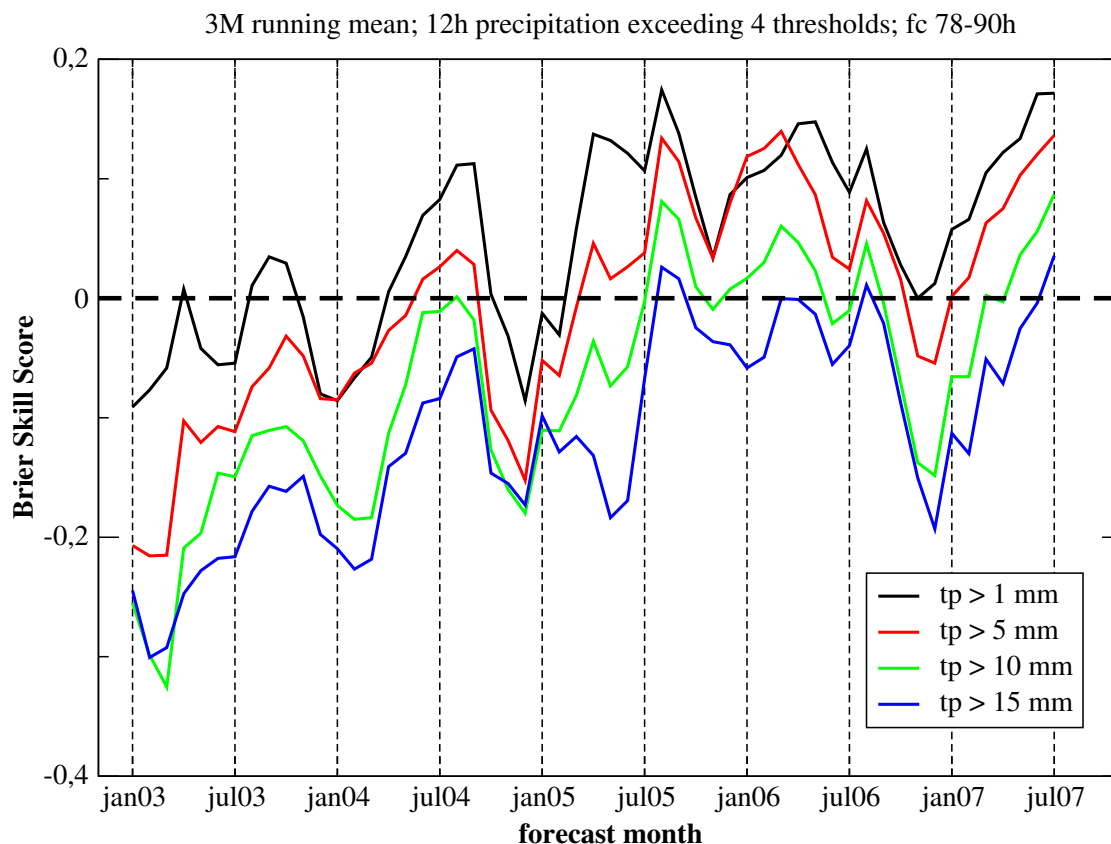


Figure 3: Brier Skill Score of COSMO–LEPS 12-hour precipitation forecasts for the forecast range 78–90h. The BSS was computed for each month, from January 2003 to July 2007. A 3-monthly running mean was applied to the scores to improve the readability.

As an example of the obtained results, Fig. 3 shows the performance of COSMO–LEPS in terms of the Brier Skill Score (BSS), for 4 different thresholds (1, 5, 10, 15 mm/12h) at the 78–90h forecast range. Although the score is computed monthly, the 3-month running mean is actually shown in the plots to increase readability, due a marked month-to-month variability of the score itself. At the beginning of the verification period (early 2003), the BSS was always negative, increasing to positive values at least for the lower thresholds starting from summer 2004. The BSS is steadily positive from spring 2005, for all the thresholds except the highest (15mm/12h). A different behaviour is exhibited in autumn 2006, which was a very dry season: COSMO–LEPS performance is not satisfactory. On the other hand, the BSS is almost always above zero throughout 2007, indicating a skillful system in the prediction of precipitation at the day–4 range. A marked seasonal variability is also evident, the system often performing better in the summer season.

In the overall evaluation of the system performance, it has to be kept in mind that, in addition to the upgrades in the COSMO–model itself, COSMO–LEPS configuration was subject to two major changes during the verification period:

- June 2004: the ensemble members were increased from 5 to 10 and only two EPS instead of three were considered to select the global-model members to drive the COSMO-LEPS integrations;
- February 2006: the ensemble members were increased from 10 to 16 and the vertical resolution of COSMO-LEPS integrations from 32 to 40 levels.

The former change seems to have led to better scores, since an improvement is evident from spring 2004. The impact of the latter change is more difficult to be judged, due to the already underlined problem in autumn 2006. Nevertheless, a positive trend is evident in the scores obtained during 2007, especially in view of the various meteorological experiments which took place during that year (e.g. COPS and MAP D-PHASE). This is even more true if other scores, like the area under the ROC curve and the percentage of outliers, are considered (not shown).

As a final remark, it has to be pointed out that nowadays COSMO-LEPS forecast products are well-established in met-ops rooms across COSMO community. They have been recently used with success in EC projects (e.g. Windstorms PREVIEW) as well as in the field campaigns of the above-mentioned meteorological experiments. As future developments, it is planned to introduce more model perturbations, so as to improve the spread-skill relationship of the system, and to develop “calibrated” COSMO-LEPS forecasts.

## References

- Marsigli C., Montani A., Nerozzi F., Paccagnella T., Tibaldi S., Molteni, F., Buizza R., 2001. A strategy for high-resolution ensemble prediction. Part II: limited-area experiments in four Alpine flood events. *Quart. J. Roy. Meteor. Soc.*, **127**, 2095–2115.
- Marsigli C., Boccanera F., Montani A., Paccagnella T., 2005. The COSMO-LEPS mesoscale ensemble system: validation of the methodology and verification. *Nonlin. Proc. Geophys.*, **12**, 527–536.
- Montani A., Capaldo M., Cesari D., Marsigli C., Modigliani U., Nerozzi F., Paccagnella T., Tibaldi S., 2003. Operational limited-area ensemble forecasts based on the ‘Lokal Modell’. ECMWF Newsletter No. 98. Available from: ECMWF, Shinfield Park, Reading RG2 9AX, UK.

## The COSMO–SREPS Priority Project: The Autumn 2006 Testing Period

CHIARA MARSIGLI, ANDREA MONTANI AND TIZIANA PACCAGNELLA

*ARPA-SIM, Bologna, Italy*

FLORA GOFA AND PETROULA LOUKA

*HNMS, Athens, Greece*

### 1 Introduction

The development of COSMO–SREPS (COSMO Short-Range Ensemble Prediction System) is carried out within a Priority Project of the COSMO Consortium (the project description can be found at <http://cosmo-model.cscs.ch/content/tasks/priorityProjects/sreps/default.htm>). COSMO-SREPS is built to fulfil some needs that have recently arisen in the COSMO community:

- to have a short-range mesoscale ensemble to improve the support to the forecasters, especially in situations of high impact weather;
- to have a very short-range ensemble for variational data assimilation purposes (1D-Var), to estimate a flow-dependent error covariance matrix;
- to provide initial and boundary conditions to the very high resolution ensemble COSMO-DE-EPS under development at DWD.

In order to accomplish these purposes, ensemble perturbations are required to generate a reasonable spread in the short-range and to act on the spatial scales which are more affected by errors in the short-range predictions. The strategy to generate mesoscale ensemble members proposed by this project tries to take into account several possible sources of uncertainty and thus to model many of the possible causes of forecast error (Marsigli et al., 2006).

In order to take into account the error of the global model on which the mesoscale one is nested, a multi-model approach is adopted. The MUlti-Model MUlti-Boundaries (MUM-MUB) ensemble system currently run by INM (Garcia-Moya et al., 2006), where five different limited-area models (UM, HIRLAM, HRM, MM5, COSMO) are driven by four global models (IFS, GME, UM, NCEP) having different assimilation cycles, is used to provide both initial and boundary conditions. In particular, INM provides to the COSMO partners the four 25-km COSMO runs nested on the four different global models.

In the current COSMO–SREPS setup, the four INM–COSMO runs are then used to drive 16 COSMO runs at higher resolution (10 km). Each of the 25-km COSMO runs provides initial and boundary conditions to four 10-km COSMO runs, differentiated by four different model perturbations (Fig. 1). Perturbations to the model are applied in two ways: (1) using different parameterisation schemes and (2) perturbing the parameters of the schemes. The reasons leading to the choice of the perturbation of type (1) are based on the difficulty to establish which scheme is better able to parameterise a particular physical process or to approximate the true solution. As for perturbation type (2), this choice is due to the fact that a number of parameters are included in the COSMO formulation, especially in the schemes used for

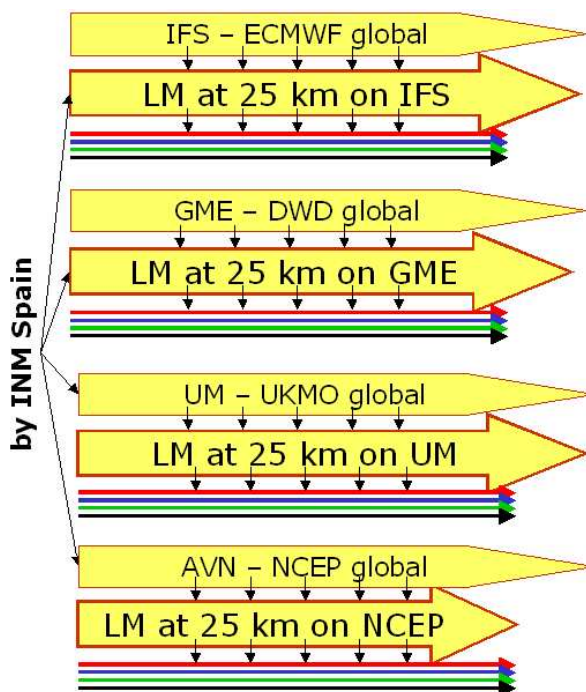


Figure 1: Scheme describing the COSMO-SREPS setup.

Table 1: Model perturbations used in COSMO-SREPS.

Name	Description	Parameter range	Default value	Used value
T	scheme for the parametrisation of the deep convection	T, KF, KFB	Tiedtke	Tiedtke
KF	scheme for the parametrisation of the deep convection	T, KF, KFB	Tiedtke	Kain-Fritsch
pat_len	length scale of thermal surface patterns	[0,10000]m	500	10000
tur_len	maximal turbulent length scale	[100,1000]m	500	1000

the parameterisations of the unresolved physical processes. Generally, these parameters are assigned a fixed value chosen within a range, which describes the uncertainty around the best estimate of the parameter. Therefore, model perturbations can be applied by varying within its range the value assigned to the parameter in the different model runs. For this purpose, the range of variability needs to be carefully specified and it is made available by the scientists involved in the development of the schemes.

The model perturbations applied to the present configuration of COSMO-SREPS are described in Table 1.

Each 25-km COSMO integration drives four 10-km COSMO runs, each of them with a different setup of the physics, i.e. the first using the Tiedtke scheme for the parametrisation of the deep convection and the default value for each of the other parameters, the second using the Kain-Fritsch scheme and the default value for each of the other parameters, the third using the default Tiedtke scheme but using the value 10000 for the pat\_len parameter and the default value for the tur\_len parameter, the fourth using the default Tiedtke scheme, the

default value for the `pat_len` parameter, but using the value 1000 for the `tur_len` parameter. Therefore, each run is perturbed only in one parameter or scheme. This allows to have four runs for each model perturbation, driven by all possible global models.

The system has been built in this way in order to permit an evaluation of the performance of the different global models as driving models and of the different physics setup. In principle, all the model perturbations have to be equivalent from a statistical point of view. A model setup which is always performing better or worse than the others should be always or never used into the model and not considered as a possible perturbation. Whether this equivalence holds, is being checked on the basis of the system runs on the testing periods.

COSMO-SREPS has been run in the described configuration over 21 cases of moderate and intense precipitation occurring over either Italy or Germany during Autumn 2006. The runs have started either at 00 or at 12 UTC, depending on the boundary conditions availability. The system runs over the same area as the COSMO-LEPS system, at a horizontal resolution of about 10 km and with 40 vertical levels. The considered forecast range is 72 hours.

A preliminary analysis of the system performance is presented here, based on this testing period.

The involvement of the Hellenic National Meteorological Service (HNMS) in Task 6 of COSMO-SREPS focused on the verification of COSMO ensemble forecasts for autumn 2006. In particular, the 21 cases of 72-hour forecast horizon and 16 members were used for verification over Greece using the available SYNOP data. The parameters verified were the 2m air temperature, the mean sea-level pressure (MSLP) and the precipitation.

## 2 Spread-Error Relationship

In order to evaluate if the perturbations applied to the ensemble are appropriate for the short-range and for the description of the uncertainty affecting the forecast of surface variables, the spread of the COSMO-SREPS system is analysed.

In Fig. 2 the COSMO-SREPS spread and error (root-mean-square), computed in terms of 2m temperature over a set of about 900 stations covering northern Italy, are compared with COSMO-LEPS one. The observations on station points are compared with the values forecasted on the nearest grid points.

Only the COSMO-SREPS runs starting at 12 UTC (7 days) have been used for this analysis, since only these runs permit a clean comparison with COSMO-LEPS, which runs every day at 12 UTC. A comparison of the 00 UTC COSMO-SREPS with the 12 UTC COSMO-LEPS seemed not to be advisable due to (1) the dependence of the spread and of the error of the time of the day and (2) the different performances of the COSMO model when driven by the 00 or the 12 UTC IFS runs.

It appears from the plot that COSMO-SREPS spread is greater than COSMO-LEPS one for the considered forecast range, being almost double during the first 24 hours and then approaching the other with increasing forecast range. This indicates that the short-range ensemble can really benefit of a source of uncertainty which plays a role in the short range. Furthermore, the errors of the two systems are quite close, suggesting that the greater amount of spread shown by COSMO-SREPS is not worsening the forecast, but permits to describe part of the uncertainty affecting the forecast, at least for the first two days.

It has to be pointed out that the error is, for both systems, higher than the spread, suggesting that both systems are underdispersive for all the forecast ranges. This is probably indicative

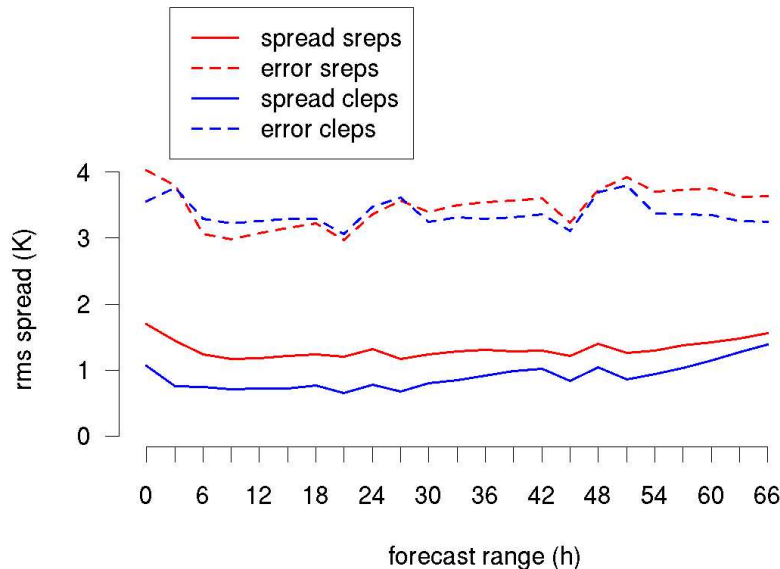


Figure 2: Root-mean-square error (dashed lines) and Root-mean-square spread (solid lines) relative to COSMO-SREPS (red lines) and COSMO-LEPS (blue lines) in terms of 2m temperature with increasing forecast range.

of the fact that the COSMO model systematic error plays a significant role, the model perturbations applied to COSMO-SREPS being probably not enough, in terms of processes described, to take it into account.

In order to address the problem of understanding how the different perturbations applied to COSMO-SREPS contribute to determine its spread, the spread has been computed also for eight different grouping of the 16 ensemble members, containing 4 members each. The members can be distinguished either on the basis of the driving run, which permits to create 4 groups labelled with the name of the driving model (ecmwf, gme, avn, ukmo), or on the basis of the COSMO model perturbation, which permits to create 4 groups labelled with p1 (T, see Table 1), p2 (KF), p3 (pat\_len) and p4 (tur\_len). The spread so obtained are plotted in Fig. 3.

For this plot, only the COSMO-SREPS runs starting at 00 UTC (14 days) have been used, due to the dependence of the spread on the time of the day.

The black line is relative to the root-mean-square distance among the 4 ensemble members which have received initial and boundary conditions from the ECMWF-COSMO run. Hence, the differences among these 4 members come only from the perturbations applied to 4 model parameters. On the other hand, the magenta line is relative to the root-mean-square distance among the 4 ensemble members which have the same model formulation, the model having been perturbed by selecting the parametrisation p2 (Kain-Fritsch) in all the 4 runs. It is clear that the spread among members having different values of physics parameters but the same driving model is always lower (almost a half) than the spread among members having different driving models but the same COSMO formulation. Therefore, the major contribution to the spread is given by the different initial and boundary conditions, as expected, on average over the whole sample. Over specific point of the domain and for specific days, the situation can be quite different and even reversed (not shown).

An evaluation of the influence of the different kind of perturbations on the error affecting

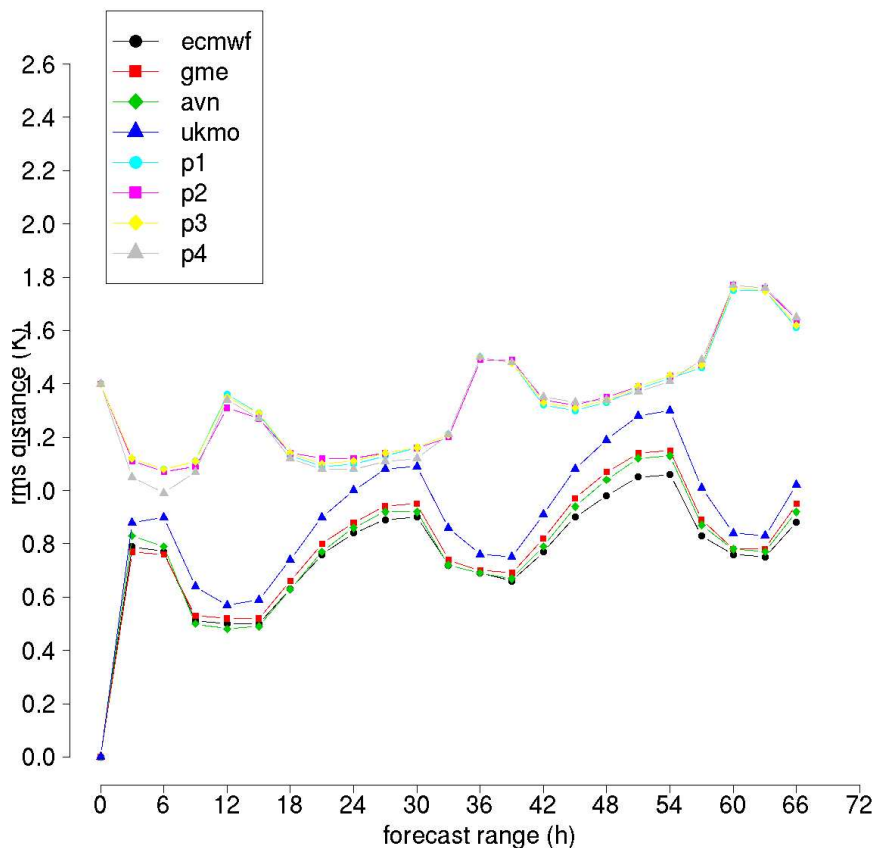


Figure 3: Root-mean-square distance, in terms of 2m temperature, among 8 different groups of ensemble members: the 4 members with the same ECMWF father in black, the 4 members with the same GME father in red, the 4 members with the same NCEP father in green, the 4 members with the same UKMO father in blue, the 4 members with the same p1 model perturbation in violet, the 4 members with the same p2 model perturbation in orange, the 4 members with the same p3 model perturbation in magenta and the 4 members with the same p4 model perturbation in cyan.

precipitation forecasts is complicated by the difficulty in defining a spread measure in terms of this parameter. In order to evaluate how the different perturbations affect precipitation forecasts, an objective verification in terms of this variable has been carried out. The skill of the COSMO-SREPS ensemble is thus compared with the skill of the eight sub-ensembles which can be built by grouping the members on the basis either of their driving model or of their physics perturbation. The ROC area values obtained for 24-h precipitation, computed by averaging both forecasted and observed values over boxes of  $0.5 \times 0.5$  degrees, are shown in Fig. 4.

Observations are provided by a dense network of raingauges covering northern Italy and Switzerland (about 1400 stations).

The two plots in the upper row show how the ROC area changes from the whole ensemble (cyan line) to each of the 4 member ensembles made up by the COSMO runs with the same driving model (blue line for ECMWF, red line for GME, green line for AVN, black line for UKMO). The reduction in score due to the difference in the number of ensemble members is evident for every sub-ensemble. Furthermore, the ROC area varies of a considerable amount

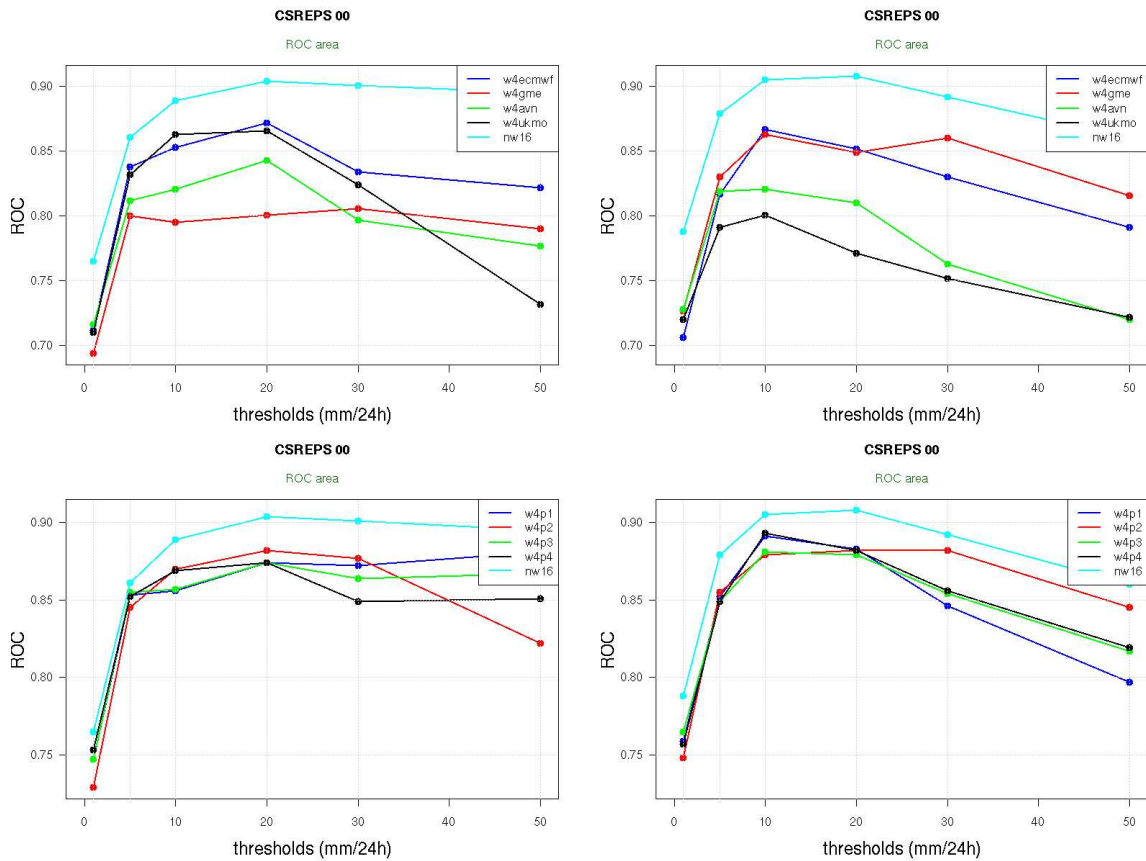


Figure 4: ROC area relative to the 24-h precipitation forecasts issued by COSMO–SREPS (cyan line) and by four sub–sets of it. In the upper panels the four sub–sets of 4 members each are made up by grouping the members with the same father, while in the lower panels by grouping the members with the same physics perturbation. The forecast range in 18–42 h in the left column and 42–66 h in the right column. Verification is performed in terms of average values over boxes of  $0.5 \times 0.5$  degrees.

from one sub–ensemble to another, the ECMWF and UKMO members performing better at the 18–42 h forecast range (left panel) while at the 42–66 h forecast range the best score is obtained by the ECMWF and GME members. These variations can also be due to the smallness of the available sample, hence, on the basis of this preliminary analysis, it is not possible to draw general conclusions about which driving model provides the best performance.

As for the 4 member ensembles made up by the COSMO runs with the same physics perturbations (lower row), the ROC area values are generally higher than those exhibited by the ensembles with the same driving model, indicating that the diversity in terms of driving model (which characterises the ensembles in the lower row) guarantees higher skill with respect to the diversity in terms of physics parametrisations alone (which characterises the ensembles in the upper row). Furthermore, the ROC areas of the 4 sub–ensembles are quite similar, indicating that all the physics perturbations are equivalent from the skill point of view.

### 3 Verification

Within the COSMO cooperation, objective verification of the COSMO–SREPS system has been carried out at HNMS (Greek National Meteorological Service), evaluating the system performance in terms of surface variables (2m temperature, precipitation, mean sea level pressure, 10m wind) over Greece. This aims also at assessing the extent to which the 16 members have different skill, depending on the driving model or on the parameter set up.

The involvement of the Hellenic National Meteorological Service (HNMS) in Task 6 of COSMO–SREPS focused on the verification of the ensemble forecasts for autumn 2006. In particular, the 21 cases of 72-hour forecast horizon and 16 members were used for verification over Greece using the available SYNOP data. The parameters verified were the 2m air temperature, the mean sea-level pressure (MSLP) and the precipitation.

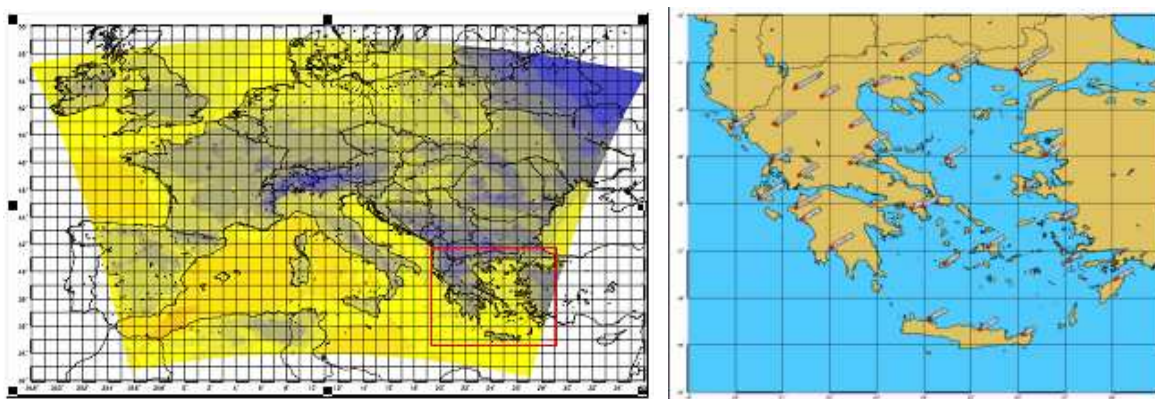


Figure 5: Left panel: the red square indicates the verification domain used for Greece. Right Panel: the SYNOP stations.

Greece is located at the very southeast part of the domain implemented (Fig. 5, left panel), therefore some SYNOP data may be influenced by the boundaries. 30 stations were used for the verification as shown in the right panel of Fig. 5. Due to the complexity of Greece's topography the grid points closest to the location of the stations were used.

For the continuous parameters of temperature and MSLP the statistical analysis was based on the calculation of Bias and Root Mean Square Error (RMSE) averaged over all forecast members and stations. Fig. 6 shows the results of the statistical analysis for all forecast members. In general, averaged BIAS and RMSE values showed a small overestimation of MSLP (not shown) and statistically acceptable values, namely, approximately 2C for 2m temperature and less than 5 mb for MSLP (Fig. 6), apart from a few specific forecasts in November for which RMSE was large compared to the mean value (Fig. 7).

The verification of the 6-hour precipitation, being a non-continuous parameter, was based on the deterministic approach, namely, the production of contingency tables, the calculation of the Probability Of Detection (POD), the False Alarm Rate (FAR) and other statistical scores. The threshold ranges used for these quantities were: 0-0.1 mm, 0.1-4.0 mm, 4.0-9.0 mm, >9.0 mm. These values were lower than those conventionally used in SREPS due to the limited precipitation amounts existing during the selected period.

The sample used was statistically small for extracting conclusive information on precipitation forecast. Figure 8 shows the evolution with forecasting period of POD and FAR grouped according to the different initial conditions for the two first threshold ranges. Figure 9 shows the same results but grouped according to the different convective scheme parameterizations.

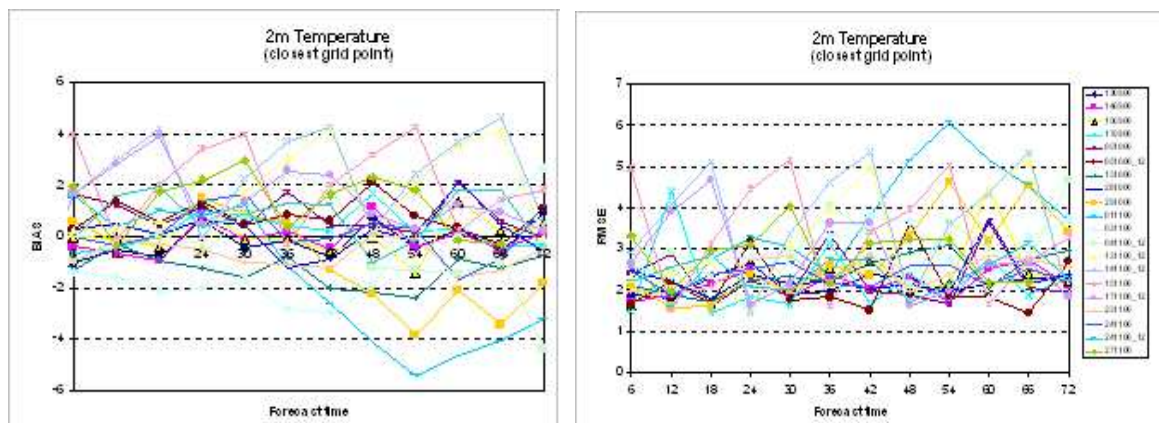


Figure 6: Bias (left panel) and RMSE (right panel) for 2m air temperature for all forecast members.

The available results suggested that the precipitation amounts were generally overestimated. The influence of the different initial conditions on the forecasted precipitation field was evident. The influence of the convective scheme and turbulent length scale is important mainly on forecasting accurately the presence of a precipitation event as indicated by the POD value.

#### 4 Summary and Outlook

The analysis of the COSMO–SREPS performances for the Autumn 2006 testing period permits to draw positive conclusions on the usefulness of the system in describing the short–range forecast error affecting surface parameters, though the system results to be underdispersive. The verification over Greece carried out by HNMS indicates that the forecast error in terms of 2m temperature and MSLP is in agreement with the error of the deterministic implementation of the model.

It has to be underlined that all these results are very preliminary, being based on a very small sample of 21 days, so it is not possible to draw robust conclusions on their basis.

In order to allow an extensive evaluation of the system, COSMO–SREPS was run during the whole DOP (June to November 2007) of the MAP D-PHASE project. The ensemble was run at the 00 UTC of each day for which the initial and boundary conditions provided by INM were available, ending in 107 runs which cover unevenly the 6 month period.

An evaluation of the spread of the system, also in relation to the forecast error, is being carried out in terms of both surface and upper air parameters (2m temperature, MSLP, Z500).

Furthermore, a study on the physics perturbations is being carried out, in order to select the most promising physics perturbations to be applied to COSMO–SREPS in the future. Since the COSMO–SREPS system has proved to be underdispersive in the first testing period, the possibility of adding more and more different physics perturbations is being explored. For this purpose, a 16 member ensemble has been running, taking initial and boundary conditions for each run from the operational IFS deterministic run and applying 16 different physics perturbations to the model. This is being done for the whole Autumn 2007 (91 runs), with the same model version and domain used for COSMO–SREPS.

Finally, the future plans of HNMS within COSMO–SREPS are:

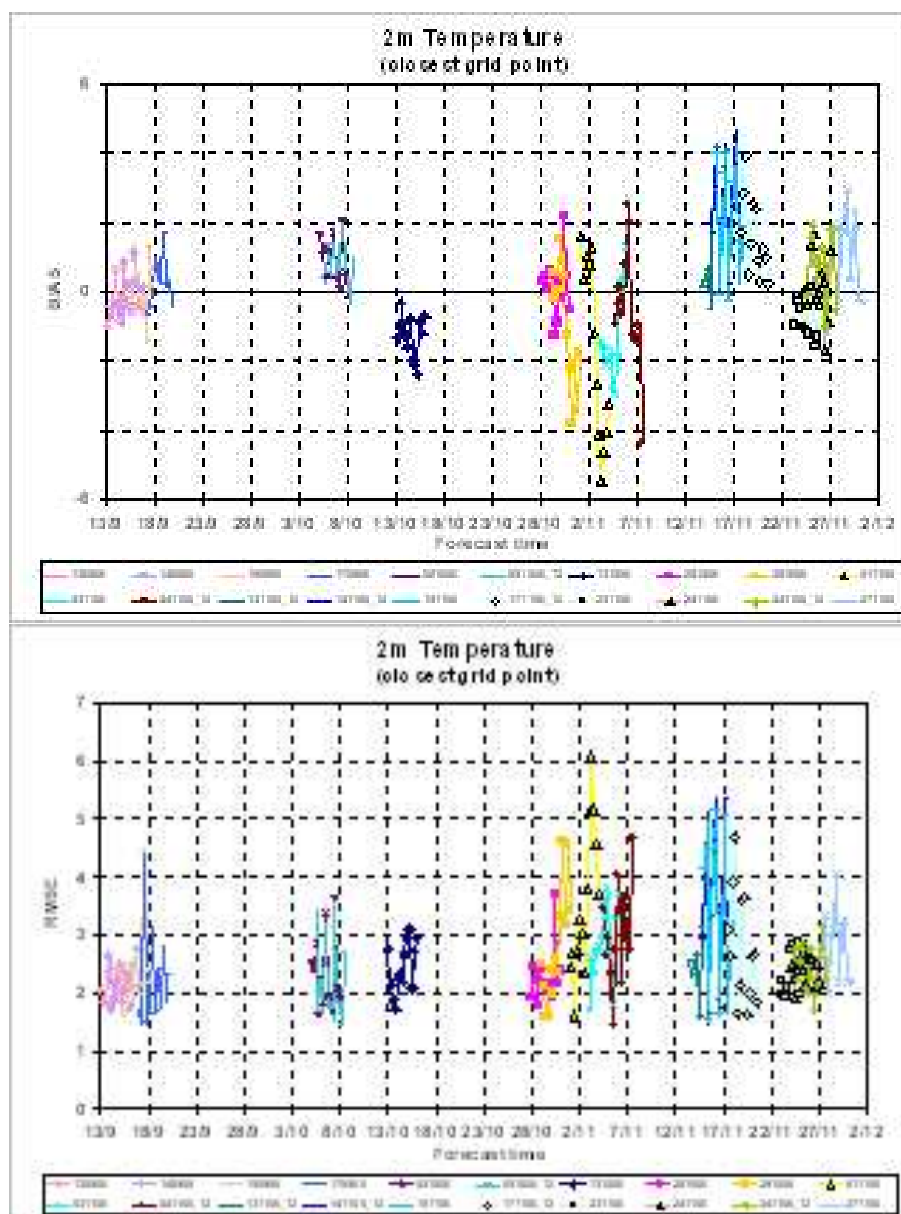


Figure 7: Bias (left panel) and RMSE (right panel) for 2m air temperature for all forecast members during the testing period.

- Application of the existing statistical methods to a larger sample (MAP D-PHASE period)
- Extend the statistics to include other meteorological parameters (wind where available)
- Investigation of precipitation ensemble forecasts using probabilistic approach (ROC diagrams, etc)

## References

Garcia-Moya, J.A., A. Callado, C. Santos, D. Santos, J. Simarro and B. Orfila, 2006: Recent Experiences with the INM Multi-model EPS scheme. *Newsletter of the 28th EWGLAM and 13th SRNWP meetings*, 9-12 October 2006, Zürich, Switzerland, 267-276.

Marsigli, C., A. Montani and T. Paccagnella, 2006: The COSMO-SREPS project. *Newsletter*

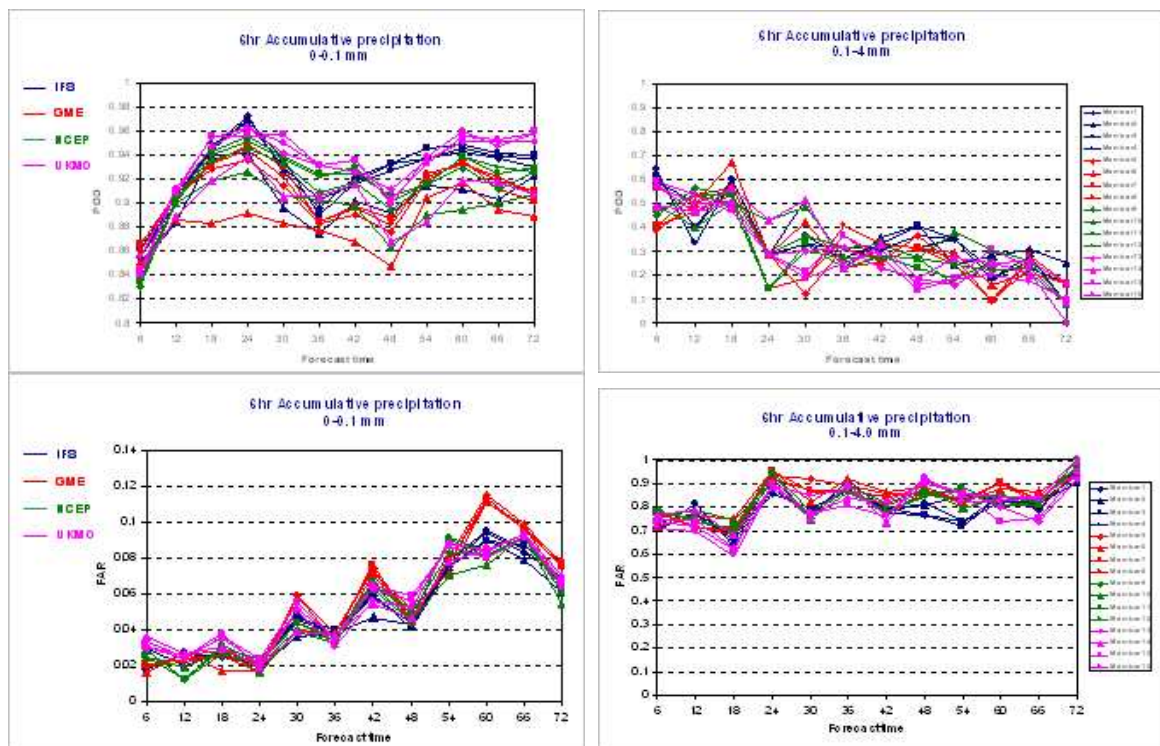


Figure 8: Values of POD and FAR grouped on different initial conditions.

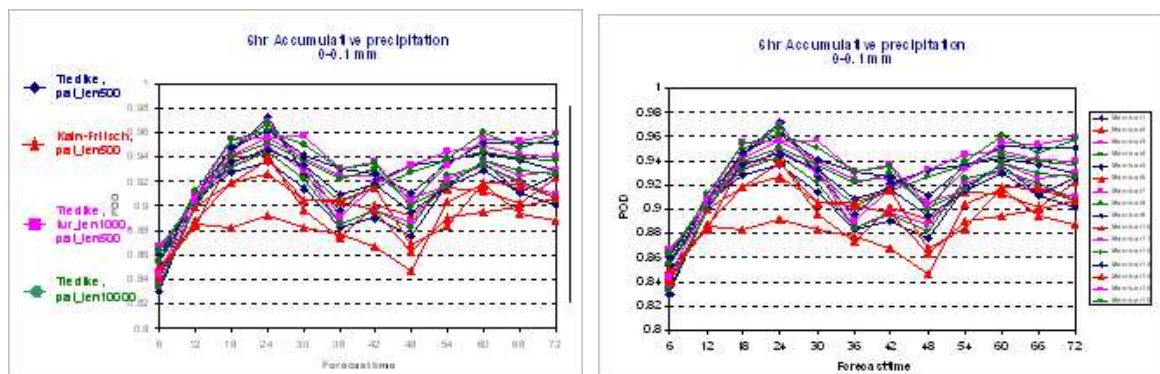


Figure 9: Values of POD and FAR grouped on different convective scheme.

of the 28th EWGLAM and 13th SRNWP meetings, 9-12 October 2006, Zürich, Switzerland, 277-283.

## Report about the Latest Results of Precipitation Verification over Italy

ELENA OBERTO, MARCO TURCO

*ARPA PIEMONTE, Torino, Italy*

### 1 Introduction

In the last year we carried out the QPF verification of the three model versions (COSMO-I7, COSMO-7, COSMO-EU) using high resolution network of rain gauges coming from COSMO dataset and Civil Protection Department (about 1300 stations). In this report we present an update of the most recent results highlighting the failures and improvements of the model: the skills and scores are calculated considering 6h or 24h averaged cumulated observed/forecasted precipitation value over 90 meteo-hydrological basins that cover all the peninsula with the exception of two Southern regions, Sicilia and Puglia (see Fig. 1).



Figure 1: Italian high resolution raingauges distribution.

### 2 Spatial distribution of the error

We plot the statistical indices over each basin to map the spatial distribution of the model error. This allows to obtain a visual verification linked both to the territory characteristics and to the orography. The following maps represent BIAS, POD and FAR over Italy for D+2 of the three model versions with respect to a fixed threshold of 10 mm/24h (statistically significant), concerning the most recent period according to the data availability, therefore

from January 2006 to August 2007. The results over Abruzzo region have not to be considered because of observed data problems. So, in Fig. 2 the BIAS is shown for the three versions: it has a quite similar pattern over North Italy, with a general overestimation over the mountain areas and an underestimation over the lowlands; over Centre and South Italy, COSMO-7 and COSMO-EU have similar behaviours with more cases of underestimation, while COSMO-I7 presents more cases of overestimation.

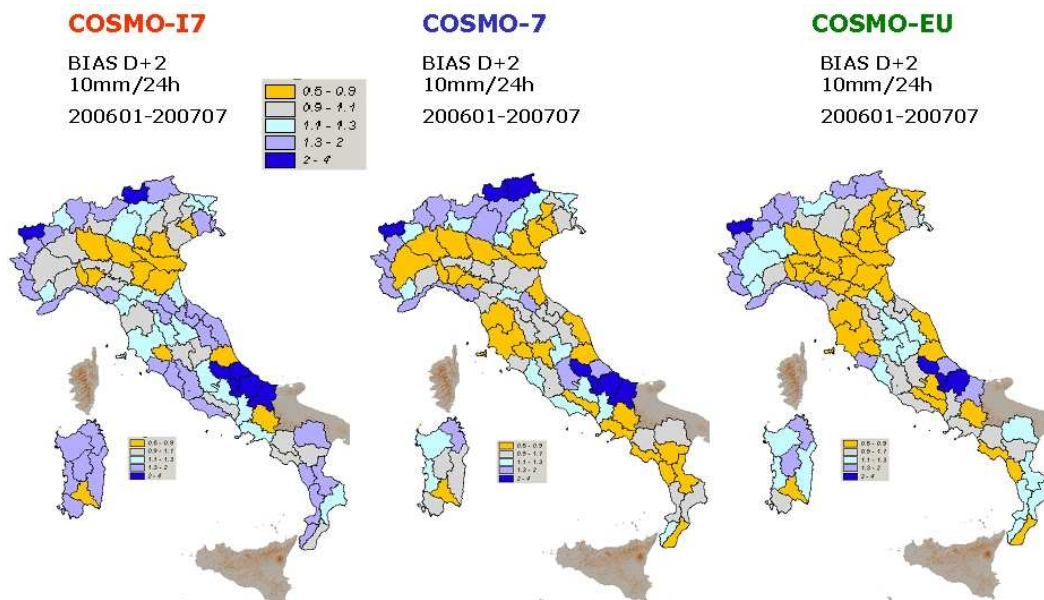


Figure 2: BIAS index over each basin for 10 mm/24h threshold (200601-200708).

Afterwards, the POD is represented in the Fig. 3: we obtain the best values in North Italy generally, but the three versions reach different skills, with very good values for COSMO-7 over alpine chain and for COSMO-EU in Northwest. In general, the East side presents the lowest values.

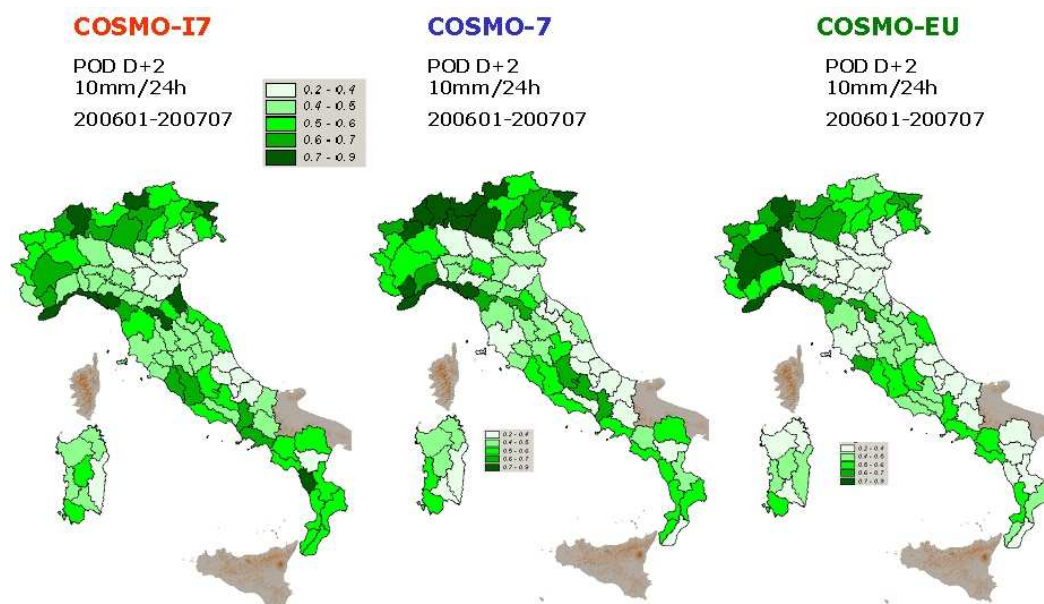


Figure 3: POD index over each basin for 10 mm/24h threshold (200601-200708).

Finally, the FAR is plotted in Fig. 4: the three versions have quite similar pattern skill, the worst values are placed in South and Centre Italy and over mountains areas. To remark the slightly more false alarm for COSMO-I7 and the slightly less for COSMO-EU.

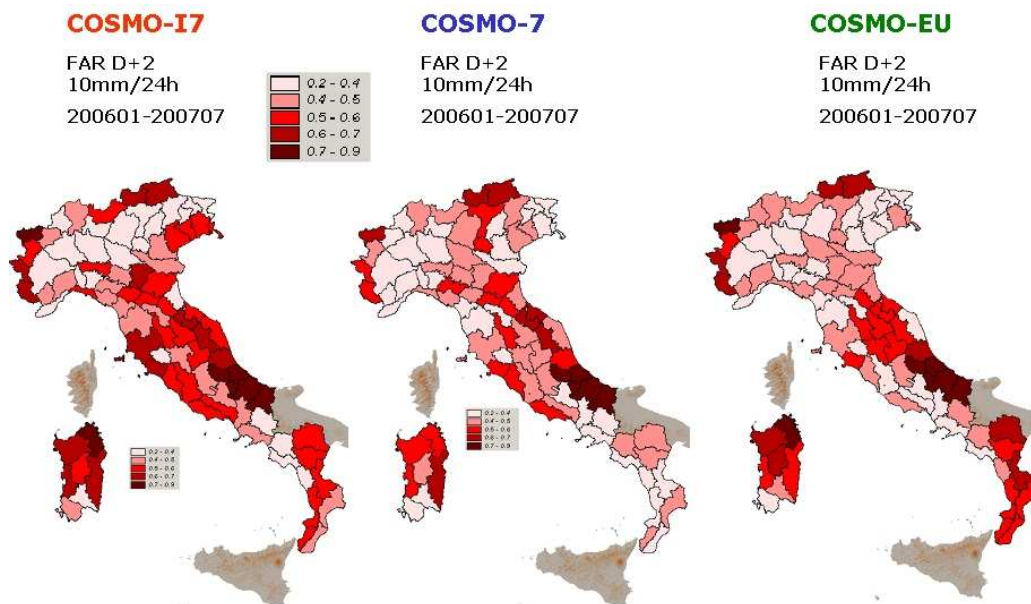


Figure 4: FAR index over each basin for 10 mm/24h threshold (200601-200708).

### 3 Seasonal comparison

In this section we analyse the performance of the three versions by a comparison among the three possible couple of the models using a bootstrap technique developed by Hamill: in order to compare two model versions, a confidence interval is necessary to assess the real differences between skill and scores and so the three versions are compared season by season in terms of BIAS, POD and FAR for a fixed threshold of 15 mm/24h. We consider the average precipitation values over each meteo-hydrogeological basin and the error bars in the following graphs indicate 2.5th and 97.5th percentiles of resampled distribution, applied to the "reference" model. Looking at Figures 5, 6 and 7 we can observe season by season the behaviour differences: in particular, COSMO-7 is most of the time better than the others, whereas the performances of COSMO-EU and COSMO-I7 are fairly equivalent. Anyway, the most relevant and remarkable result, common to all versions, is an improvement trend in the last three seasons, clearly visible in a BIAS and FAR reduction combined with a POD increase.

But we do not forget that statistical indices do not describe exhaustively the model skill: if we point out our attention to the last season (mam 2007), COSMO-EU has a very good BIAS (around 1) and it seems to performe well on average over the territory, but this is a balance effect of negative and positive errors distributed all over the territory. A very different result can be observed calculating and plotting the relative error over each basin, where underestimated/overestimated areas are highlighted (Fig. 8).

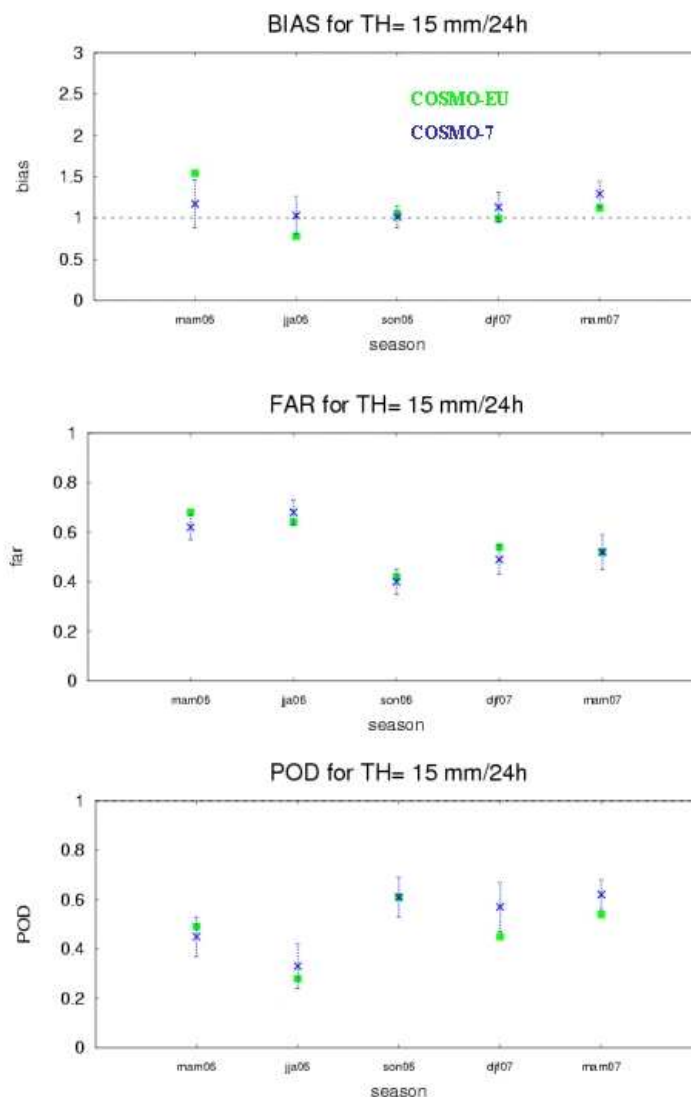


Figure 5: Seasonal comparison between COSMO-EU/COSMO-7 for D+2.

#### 4 Error diurnal cycle

We performed the error diurnal cycle considering 6h cumulated precipitation average over the basins on the period from January 2006 to August 2007 for increasing threshold (Fig. 9). We note some general remarks: the BIAS is greater than 1 (particularly for COSMO-I7) and a sort of diurnal cycle is evident with some peaks in correspondence of different forecast hours. In particular, it is noticeable how the BIAS peak occurs during midday for low thresholds, and for high thresholds it is shifted to midnight. This is an unusual result, difficult to understand. A possible explanation could be that for high thresholds the events mainly occurred during spring-summer (we have verified that) so the precipitation has a great convective component: moving from low to high precipitation amount the overestimation peak is shifted from midday to midnight, so the model seems to "see" too much instability at night during the convective events.

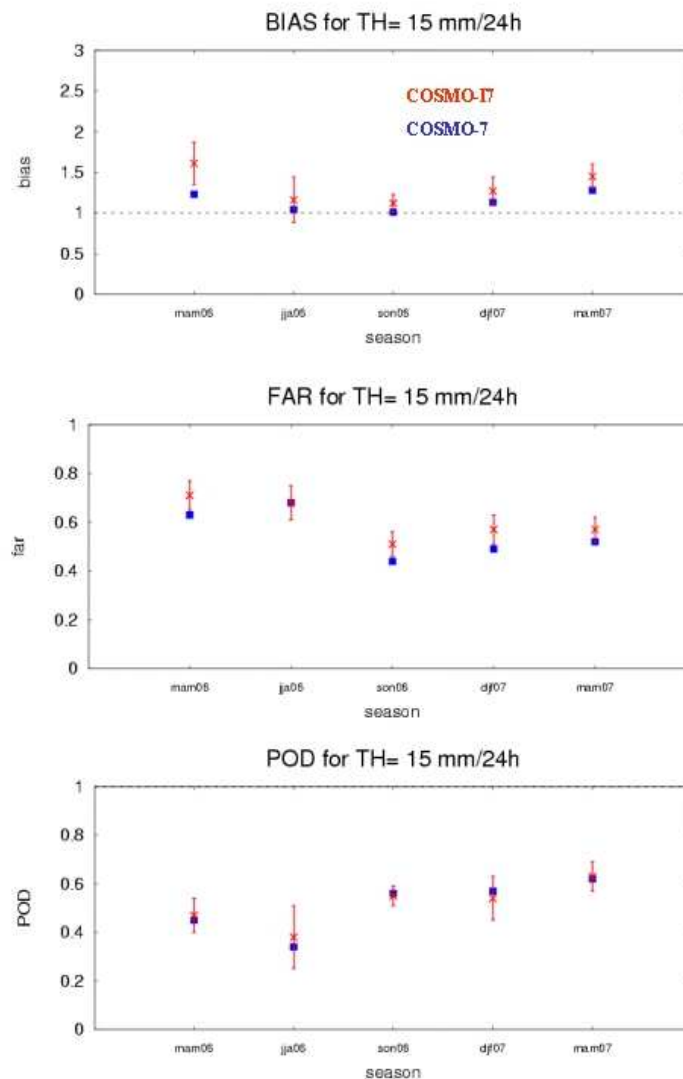


Figure 6: Seasonal comparison between COSMO-I7/COSMO-7 for D+2.

## 5 Seasonal trend over long period

Now, we focus on COSMO-I7 to evaluate the performance over a long period and to highlight the possible improvements due to the changes of the model during the years. We plot the statistical indices season by season for increasing thresholds and for D+1 and D+2 starting from winter 2003 until spring 2007: in general there is no remarkable trend, but we show the threshold 20 mm/24h because of a slightly positive trend (Fig. 10). Anyway, there is a worsening with the forecast time accompanied by a seasonal cycle with generally better skills during autumn and worse skills during summer.

## 6 Preliminary results for COSMO-I2

COSMO-I2 dissemination became operational in May 2007, so we start with a brief and preliminary verification with classical indices, BIAS, POD and FAR for D+1/D+2 over the

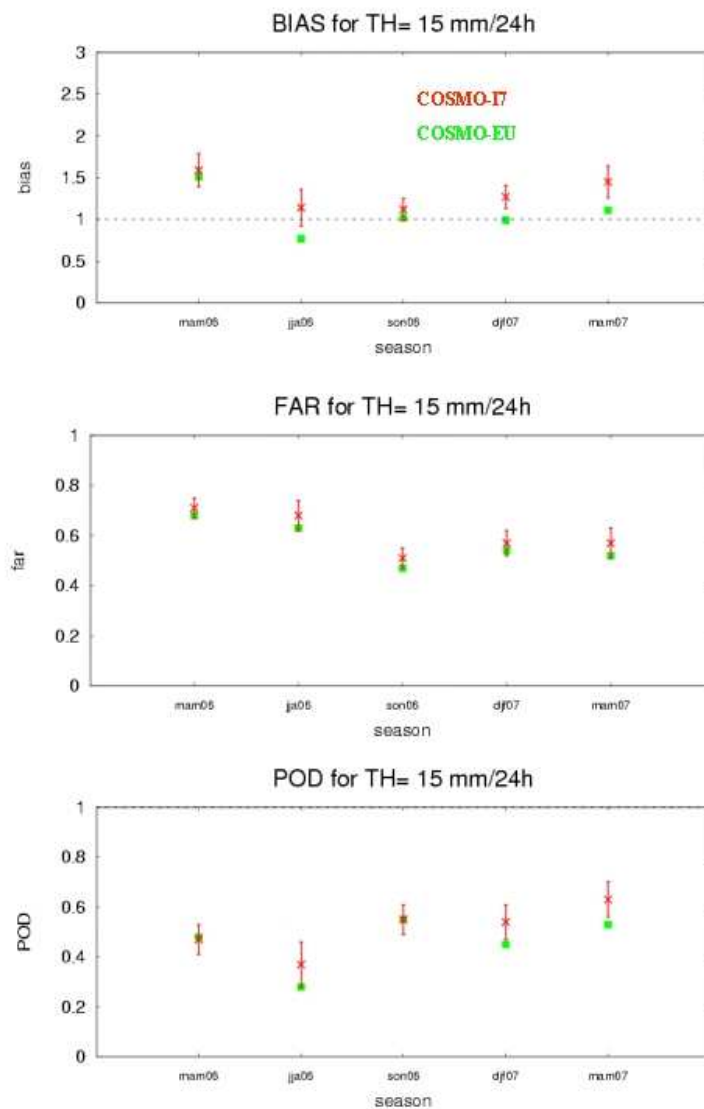


Figure 7: Seasonal comparison between COSMO-I7/COSMO-EU for D+2.

basins for increasing thresholds on a limited period of three months (200705-200707). The BIAS difference is statistically significant only for threshold above 10 mm/24h (Fig. 11), where COSMO-I2 overestimates more than COSMO-I7; on the other hand we obtain a slightly better POD for COSMO-I2 with a greater numbers of false alarms with respect to COSMO-I7 (results not shown here). According to this preliminary study, the comparison between COSMO-I7 and COSMO-I2 during the last three months shows better scores for COSMO-I7.

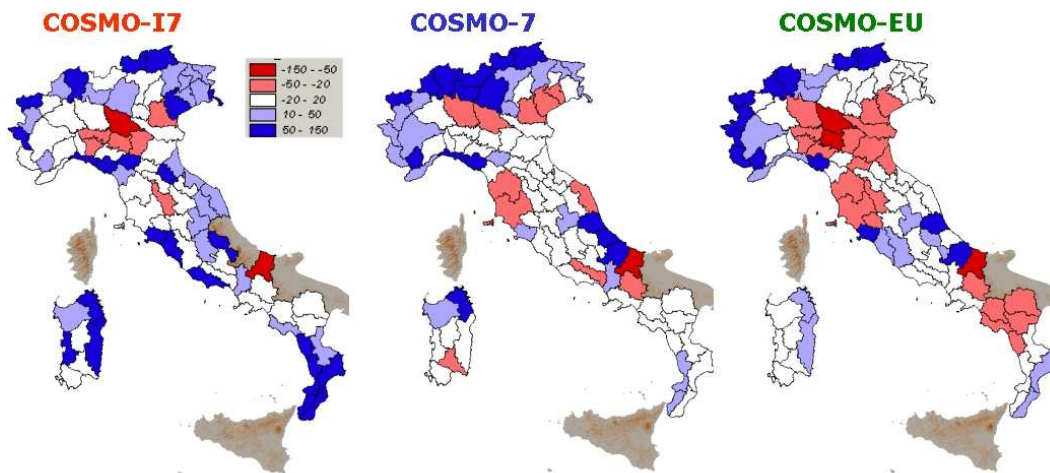


Figure 8: Seasonal comparison: relative error in mm 2007.

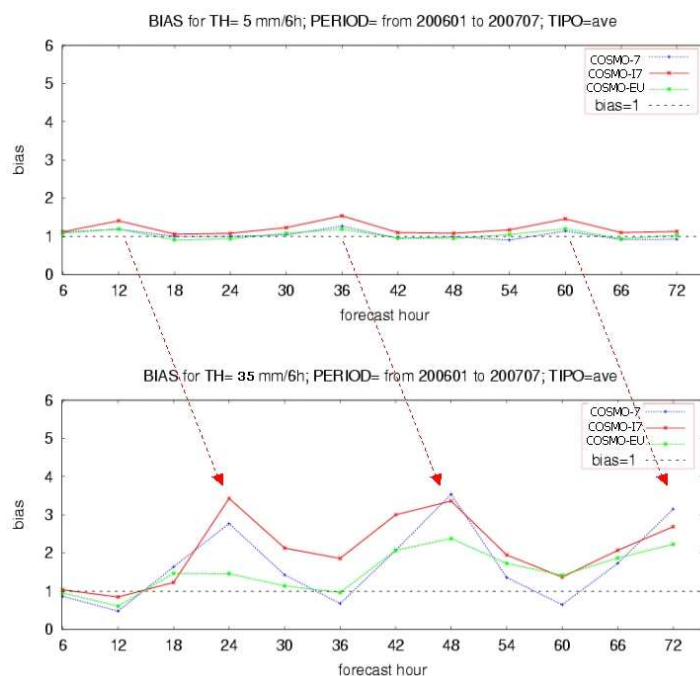


Figure 9: Error diurnal cycle for two chosen thresholds, 5 mm/6h and 35 mm/6h.

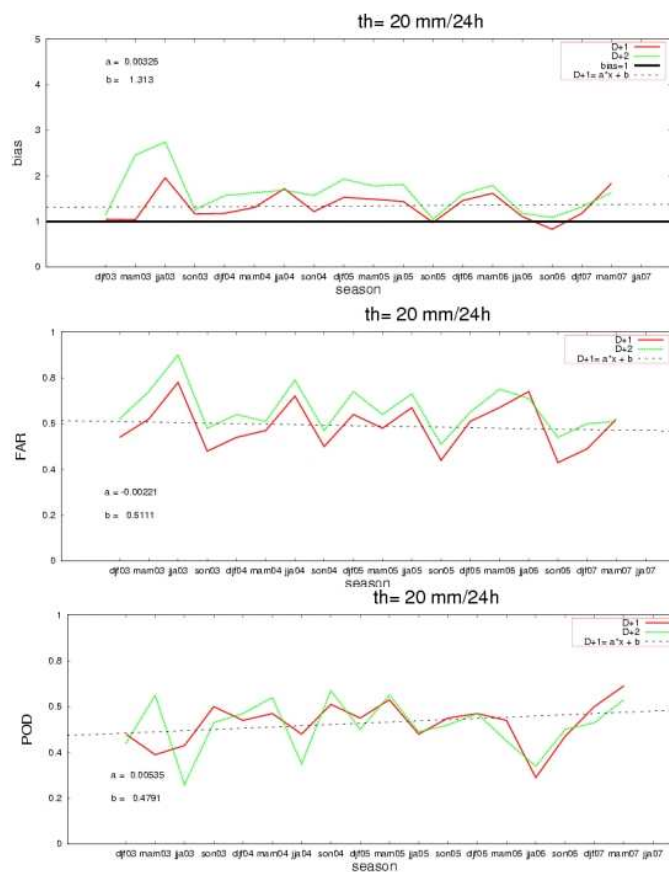


Figure 10: COSMO-I7 seasonal trend for 20 mm/24h for D+1, D+2.

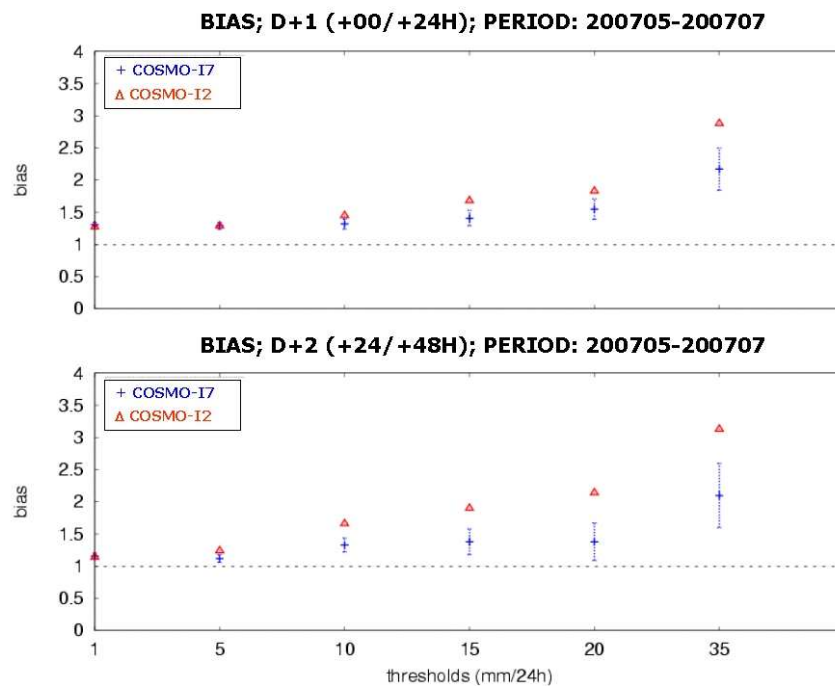


Figure 11: COSMO-I7/COSMO-I2 comparison D+1/D+2 (200705-200707).

## High Resolution Verification of COSMO-I7 2m Temperature over Emilia-Romagna Region

MARIA STEFANIA TESINI, CARLO CACCIAMANI

*ARPA-SIM Regional Hydro-Meteorological Service of Emilia-Romagna, Bologna, Italy*

### 1 Methodology and dataset

In this work we present a summary of the verification of the 2m temperature of COSMO-I7 over Emilia-Romagna region for the years 2005, 2006 and part of 2007. Comparison with other models is also shown. Configuration of COSMO-I7 operational implementation at ARPA-SIM, consisting of two 72-hour integrations every day (starting at 00 UTC and 12 UTC) with an horizontal resolution of 7 km, is summarized in Table 1.

Table 1: history of COSMO-I7 configuration

DATE	NAME (at ARPA-SIM)	MODEL VERSION	LEVELS	I.C. & B.C.	INTEGRATION DOMAIN
2005	LMSMR 2031	3.9 NUDGING	35	GME	234 × 272 pts. [domain1 in Fig. 2]
26/01/2006	LMSMR 3032	3.16 NUDGING PROG.PREC.	40	GME	234 × 272 pts. [domain1 in Fig. 2]
25/01/2007	LMSMR 4032	3.16 NUDGING PROG.PREC.	40	GME	297 × 313 pts. [domain 2 in Fig. 2]
25/01/2007	LMSMR 4032	3.16 NUDGING PROG.PREC.	40	IFS	297 × 313 pts. [domain 2 in Fig. 2]

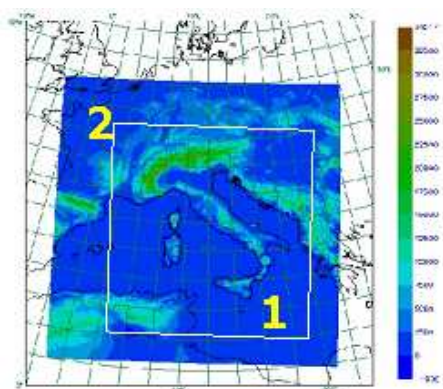


Figure 1: COSMO-I7 integration domain (before [1] and after [2] 25/01/2007)

The results have been generally computed seasonally or for shorter periods of time (e.g. two months) when model changes occurred. Verification was done with three-hourly observations

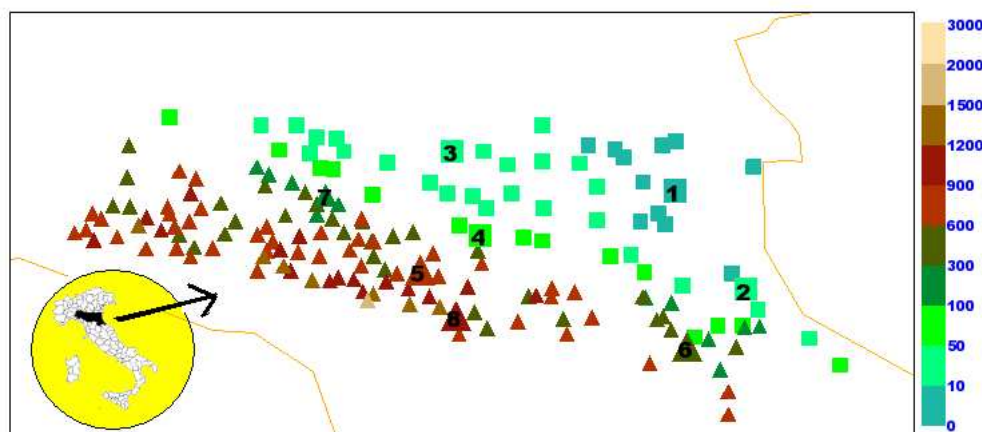


Figure 2: Emilia-Romagna ARPA-SIM observation network. Symbol colors indicate the height of the stations. Brown triangles represent mountain station (altitude >100 m) and green squares represent valley stations (altitude <100 m). Number edstation points are used in the following as a case study to show the different behavior of COSMO-I7 temperature forecast respect to the altitude of the stations.

from ARPA-SIM regional network and the nearest model grid-point. Results have been stratified depending on the altitude of the station: 56 stations below 100 m (indicated in the text as *valley stations*) and 114 above 100 m (indicated in the text as *mountain stations*). No correction for differences in height between station point and grid point has been computed and when this difference exceeds 50 m, the point was rejected. Land-sea mask has also been taken into account.

## 2 Results

Bias Error (or Mean Error) and Mean Absolute Error concerning seasonal verification of COSMO-I7 00UTC run for the year 2005, are presented in Fig. 3. A different behavior respect to the height of the stations can be observed: above 100m of altitude the model presents a negative bias during all the seasons, more pronounced in winter (up to  $-4^{\circ}\text{C}$ ). In plain region model bias varies according to the seasons: nearly zero or negative ( $-1^{\circ}\text{ircC}$ ) in winter and spring, positive in autumn and summer (up to  $3^{\circ}\text{ircC}$ ).

Concerning MAE it should be noted that in valley stations is about  $2^{\circ}\text{ircC}$  on average, with a slightly increase during midday, except in summer when an additional positive error arises during the night (up to  $3^{\circ}\text{ircC}$ ). In mountain stations there is a clear worsening of the MAE during winter (more than  $3^{\circ}\text{ircC}$  on average) and, less pronounced, in spring ( $2.5^{\circ}\text{ircC}$  on average).

It is interesting to note the quite large MAE (on average up to  $2^{\circ}\text{ircC}$ ) at the +3h forecast step and a very small trend with forecast time.

Since model version has been updated at the end of January 2006, the verification results of this year, shown in Fig. 4, refers to COSMO 3.16 with 40 vertical levels. Verification results seem to suggest a general heating of COSMO-I7 2m temperature. In mountain regions this aspect produces a significant reduction in the model MAE respect to the previous year, particularly in winter, while in valley stations COSMO-I7 seems to produce worse results. In detail, an overestimation during nighttime is observed during all seasons in valley stations,

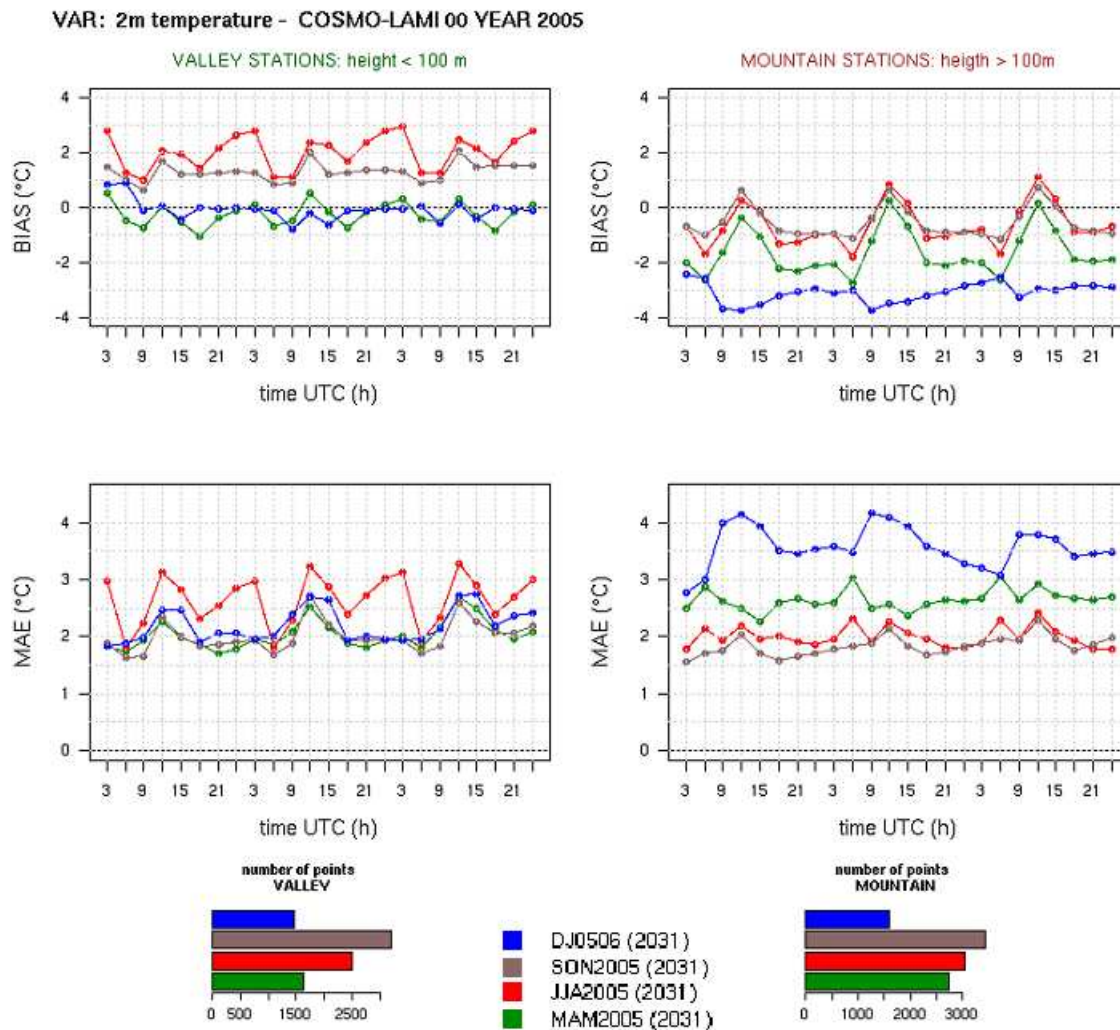


Figure 3: Bias Error (upper part) and Mean Absolute Error (lower part) for seasonal verification of COSMO-I7 (00UTC run) for year 2005. Left graphics refer to valley station (below 100m), right graphics refer to mountain stations (over 100m). The colors represent the seasons: green for spring (Mar2005–May2005), red for summer (Jun2005–Aug2005), brown for autumn (Sep2005–Nov2005), blue for winter (Dec2005–Jan2006). Barplots represent the number of points (stations × time period) used in the statistical computation.

while in 2005 this occurred only during summer. It should be pointed out that the error at the +3h forecast step (corresponding to 3UTC) is greater than  $2^{circ}C$  (up to 4C in summer) and this error seems to reflect in the daily cycle. The MAE at the last forecast time is smaller than that observed at the +3h forecast step.

Comparison with other models (features summarized in Table 2) for summer and autumn 2006 is presented in Figs. 5 and 6. It is of note that the models of the “COSMO family” show a very similar behavior concerning the daily cycle. Runs starting at 12 UTC (COSMO-I7 and LMDET) exhibit a slightly smaller error during nighttime. It is interesting to point out a difference in the +3h forecast step error between models starting at 12UTC and 00UTC. No significant difference appear between COSMO-I7 12UTC runs with nudging assimilation and the Cosmo-LEPS deterministic run (LMDET) starting at 12UTC with no assimilation.

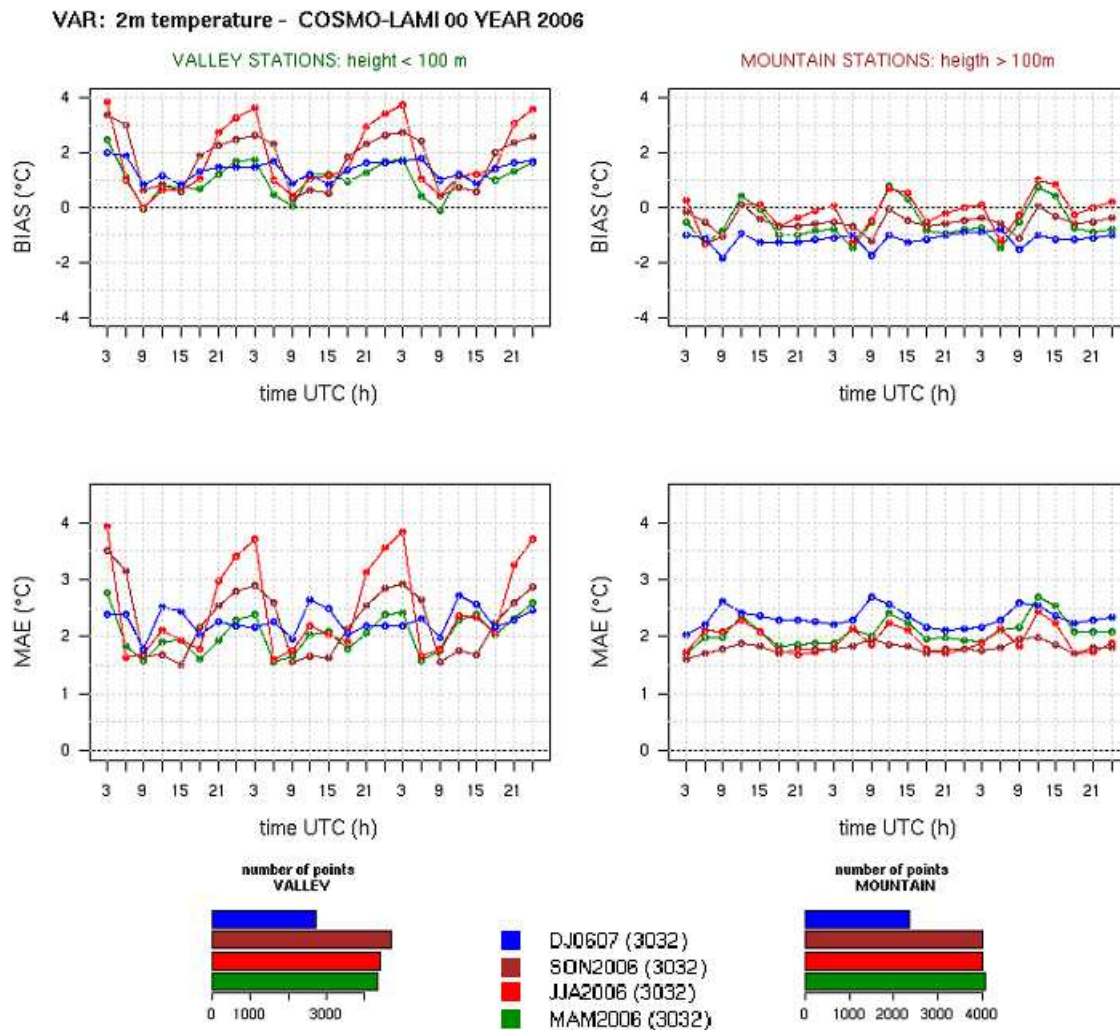


Figure 4: Bias Error (upper part) and Mean Absolute Error (lower part) for seasonal verification of COSMO-I7 (00UTC run) for year 2006. Left graphics refer to valley station (below 100m), right graphics refer to mountain stations (over 100m). The colors represent the seasons: green for spring (Mar2006–May2006), red for summer (Jun2006–Aug2006), brown for autumn (Sep2006–Nov2006), blue for winter (Dec2006–Jan2007). Barplots represent the number of points (stations × time period) used in the statistical computation.

COSMO-I7 integration domain changed at the end of January 2007 moving to a larger one (see fig.2) and since 3 April 2007 COSMO-I7 runs with boundary condition from ECMWF. For these reasons we present in Figs. 7 and 8 the verifications of two periods, February-March and April-May instead of the usual seasonal verification. The changes in domain configuration do not seem to modify the errors features pointed out in the previous year verification.

### 3 February-March 2007: a qualitative study

For the period February-March a qualitative analysis has been done graphically by drawing a scatterplot of COSMO-I7 00UTC forecast against observed temperature in valley stations

Table 2: Main features of models used for comparison

NAME (at ARPA-SIM)	MODEL FEATURES
E-SUITE (RK) LMSMR 3033	as COSMO-I7 (LMSMR 3032) with Runge-Kutta scheme run starting time: 00UTC
LMDET (reference version of COSMO-LEPS)	~ 10 km horizontal resolution 40 vertical levels I.C. & B.C.: IFS (ECMWF) NO NUDGING COSMO-LEPS integration domain run starting time: 12UTC
ECMWF	global model ~ 50 km horizontal resolution run starting time: 00 UTC & 12UTC

(Fig. 9) and in mountain stations (Fig. 10). If the forecasting system were perfect, all points would lie on a straight line that starts at the origin and has a slope of unity. While the behavior of the model concerning the observations in mountain points seems to be nearly linear, even if there is a fair amount of scatter around the ideal line, COSMO-I7 in valley points exhibits a systematic overestimation errors. It should be noted that no temperature below zero were forecasted in the period February-March 2007 despite some observed frosts.

As example in Fig. 11 is shown COSMO-I7 2m temperature forecast for the 5<sup>th</sup> of February 2007 03UTC (+3h forecast): all the Po valley has a forecasted temperate of about 3 *ircC* while observations present negative value (up to -4 *ircC* in many stations). The overestimations of 2m temperature in valley stations during nighttime can be ascribe to a wrong cloud cover forecast, but in the case shown the model correctly reproduce clear sky conditions .

Another possible source of this type of error is the relationship between 2m temperature and the first level temperature. As example, time series of forecast 2m T and lowermost T (HLD4041) of COSMO-I7 00 UTC and observed temperature in 10 stations at different altitude for the 4<sup>th</sup> and 5<sup>th</sup> of February 2007 are presented in Fig. 12 (see dataset map in Fig. 1 for the geographical position).

Further investigations are needed to understand these type of errors, in relations also with surface wind, soil moisture, heat exchange etc.

## SUMMER 2006

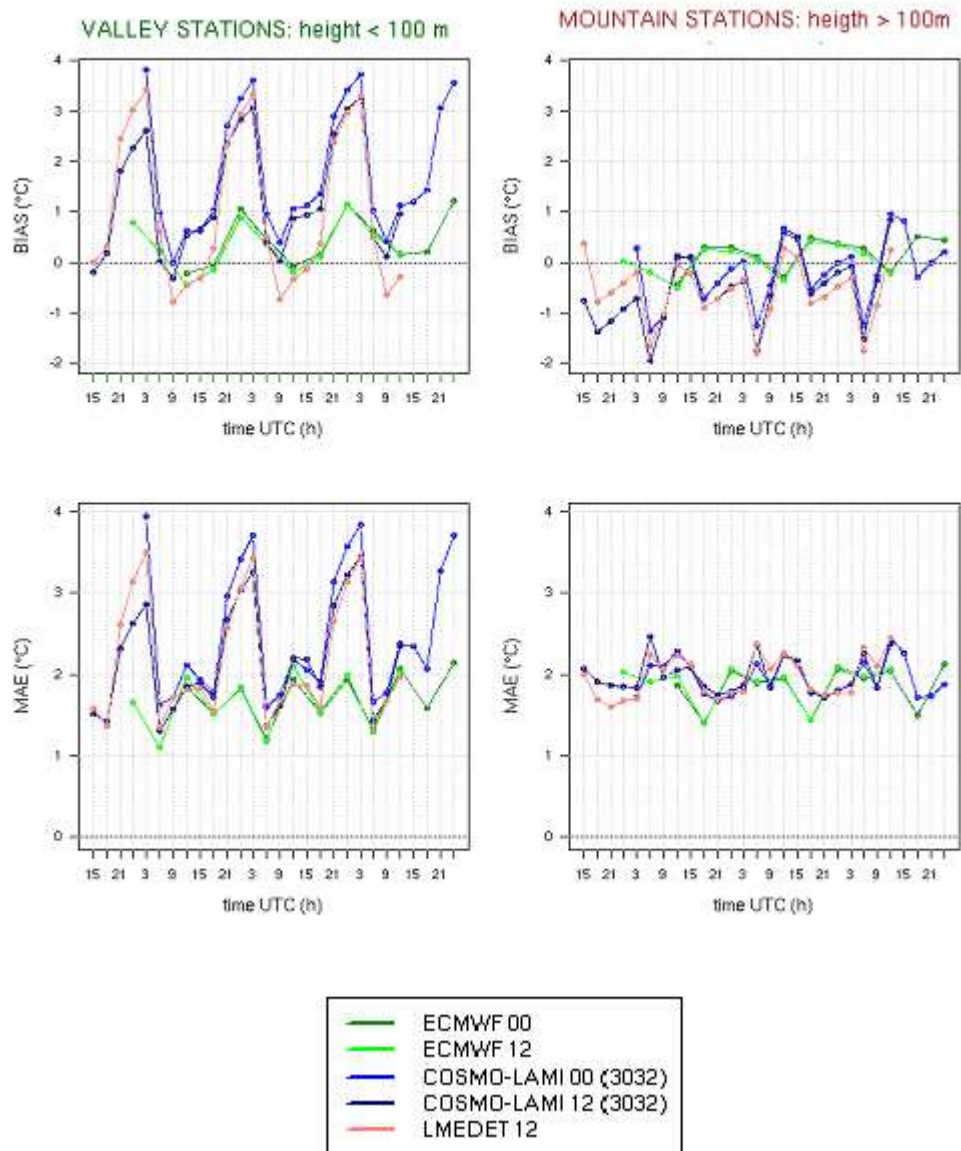


Figure 5: Comparison of summer 2006 verification of COMSO-I7 (runs 00UTC and 12 UTC), ECMWF (runs 00UTC and 12 UTC) and LMDET models. ECMWF verification has been computed using a 6h forecast step.

## AUTUMN 2006

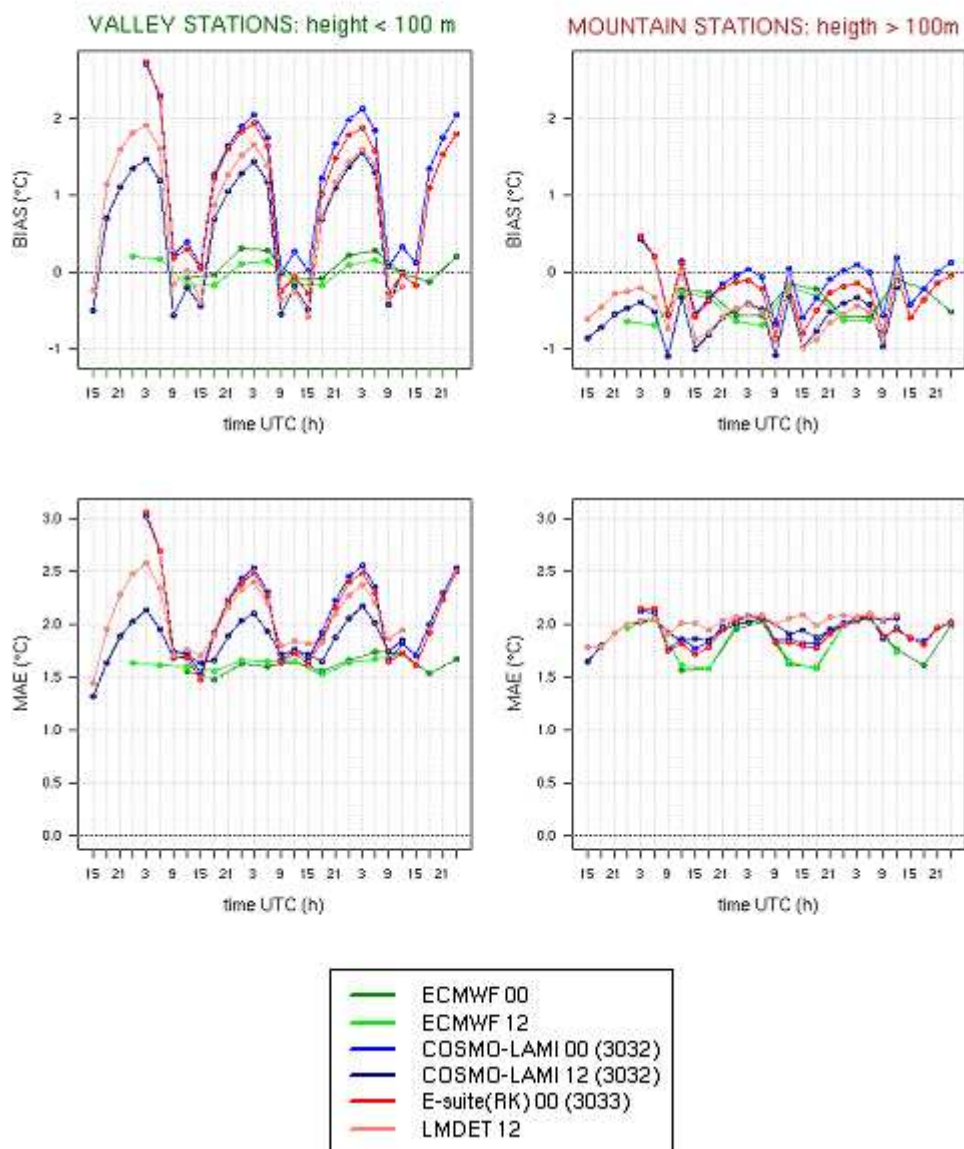


Figure 6: Comparison of autumn 2006 verification of COMSO-I7 (runs 00UTC and 12 UTC and Experimental Suite), ECMWF (runs 00UTC and 12 UTC) and LMDet models. ECMWF verification has been computed using a 6h forecast step.

## FEBRUARY-MARCH 2007

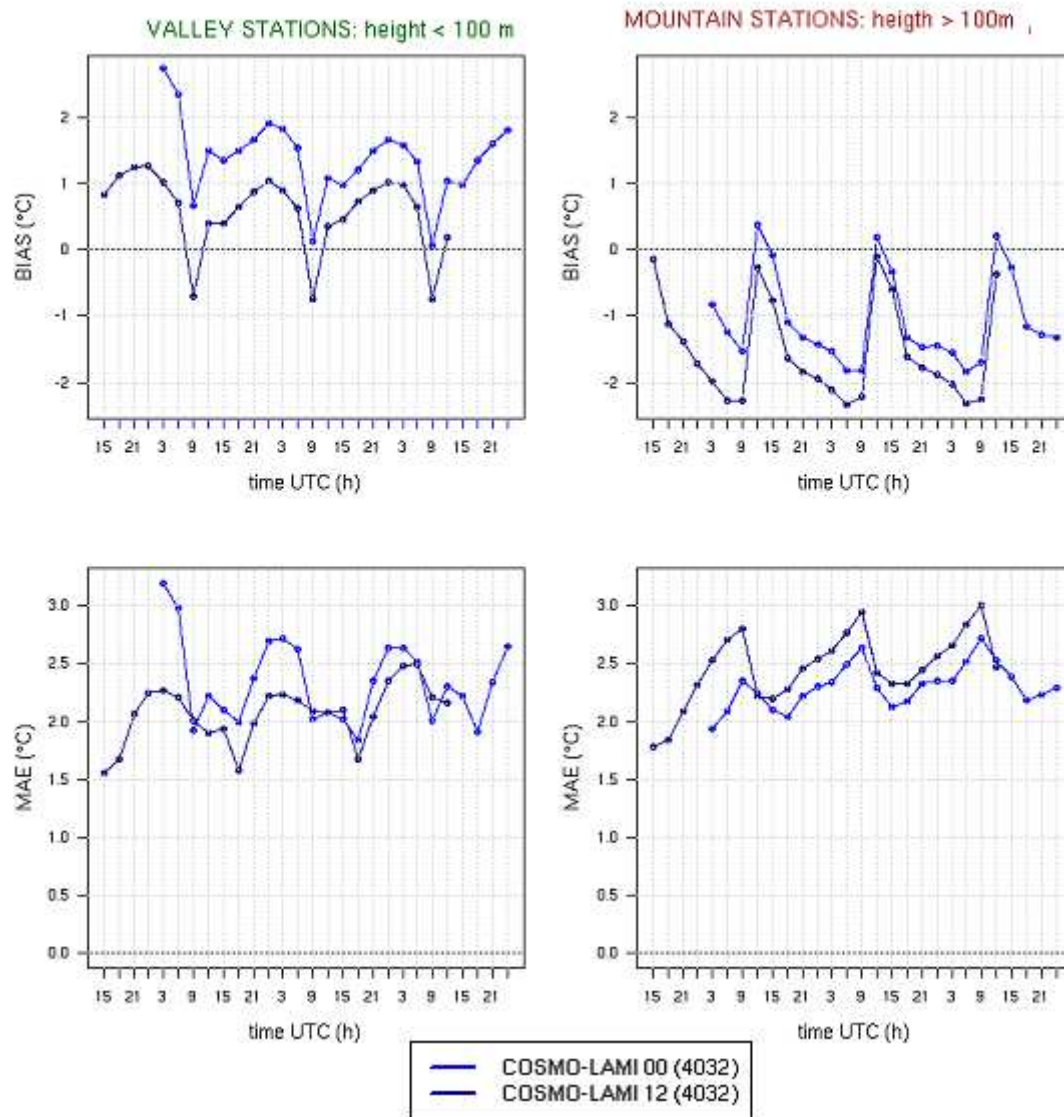


Figure 7: February-March 2007 verification results for COSMO-I7 00UTC and 12UTC runs for valley stations(left part) and mountain stations(right part)

## APRIL-MAY 2007

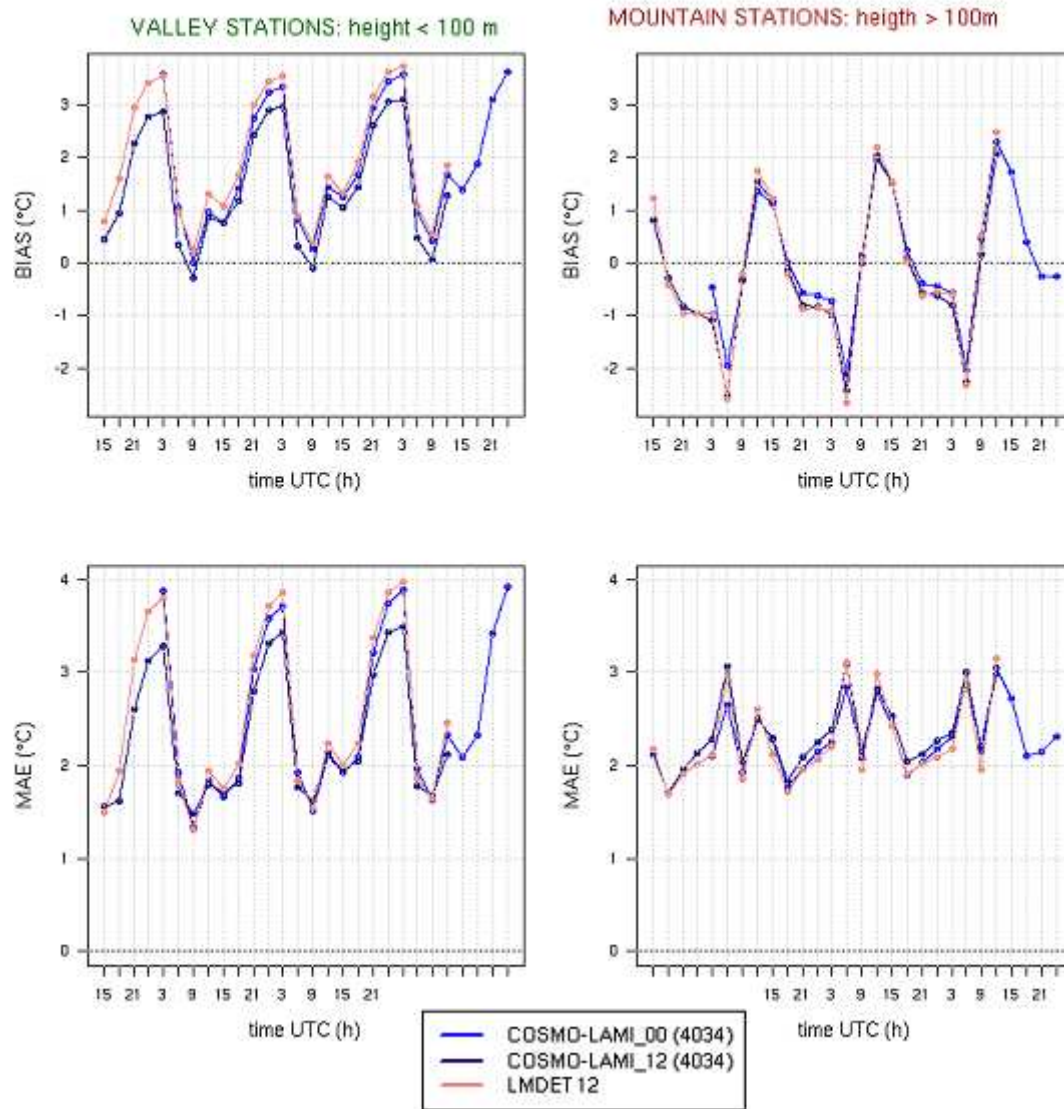


Figure 8: April-May 2007 verification results for COSMO-I7 00UTC and 12UTC runs for valley stations(left part) and mountain stations(right part)

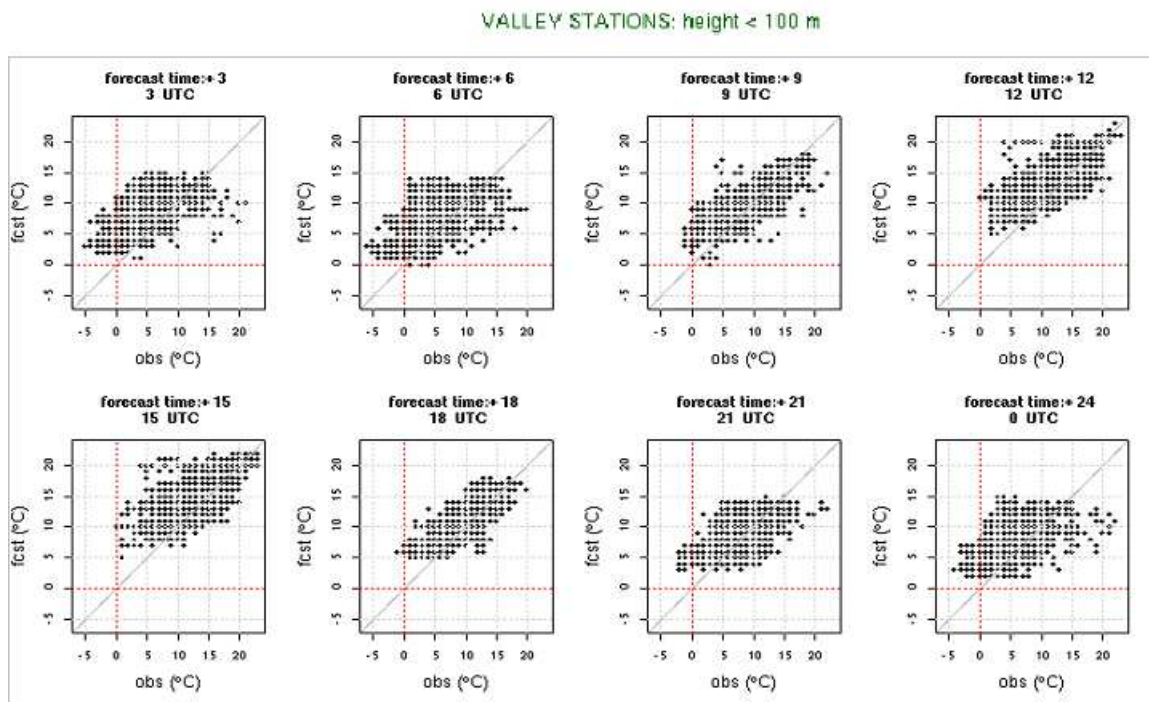


Figure 9: Scatterplot of COSMO-I7 2m temperature for valley station in the period February-March 2007 against observations. Each frame represents a forecast step (from +3h corresponding to 3 UTC to +24h corresponding to 00 UTC)

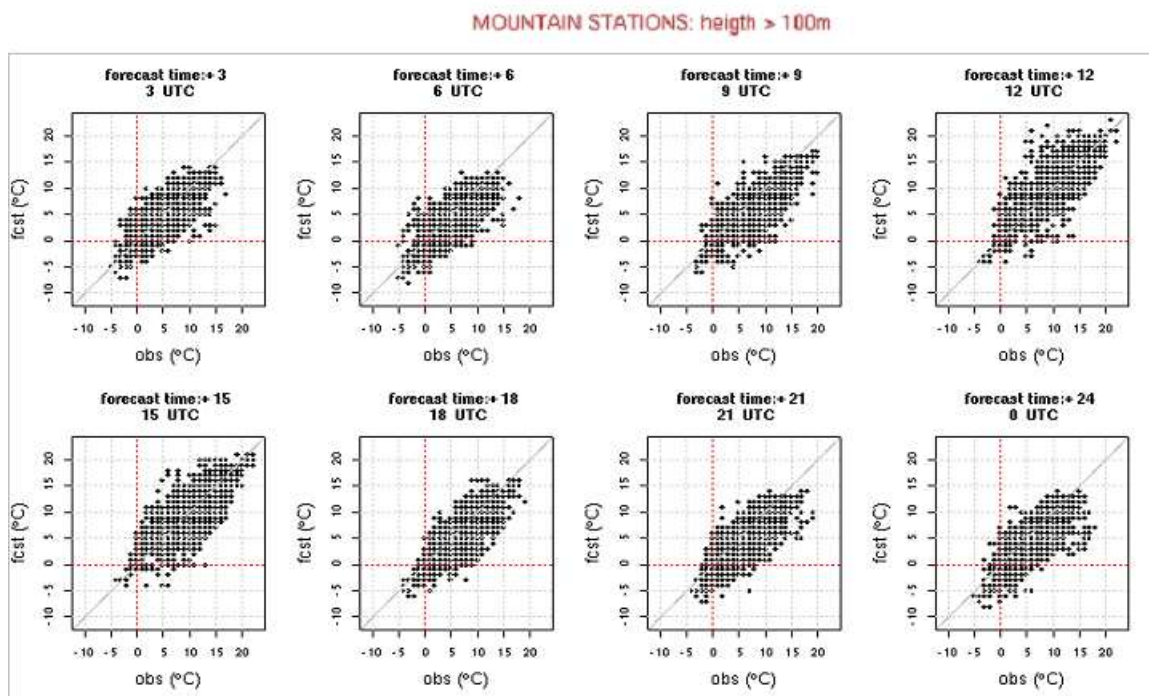


Figure 10: Scatterplot of COSMO-I7 2m temperature for mountain station in the period February-March 2007 against observations. Each frame represents a forecast step (from +3h corresponding to 3 UTC to +24h corresponding to 00 UTC)

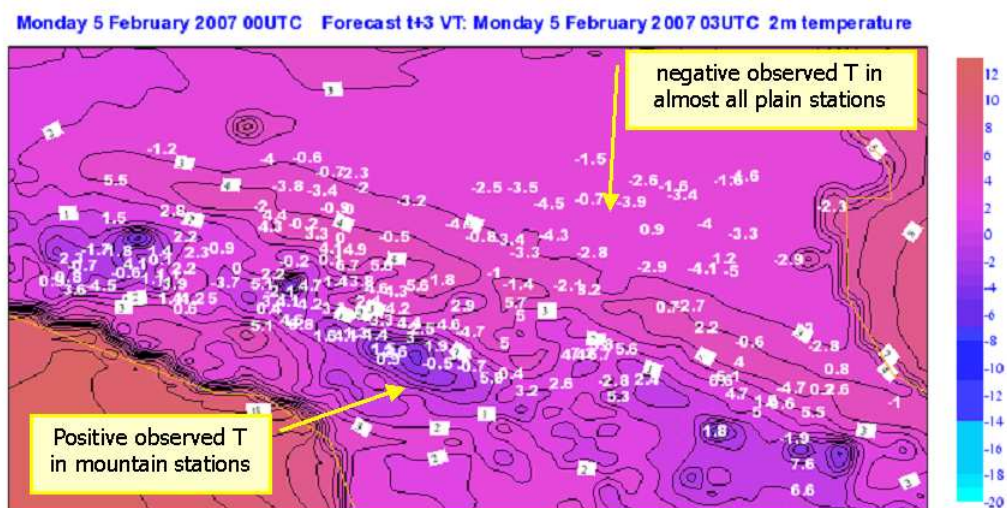


Figure 11: 5<sup>th</sup> February 2007 03 UTC: contour map of COSMO-I7 2m temperature (+3h) and observed value (in white).

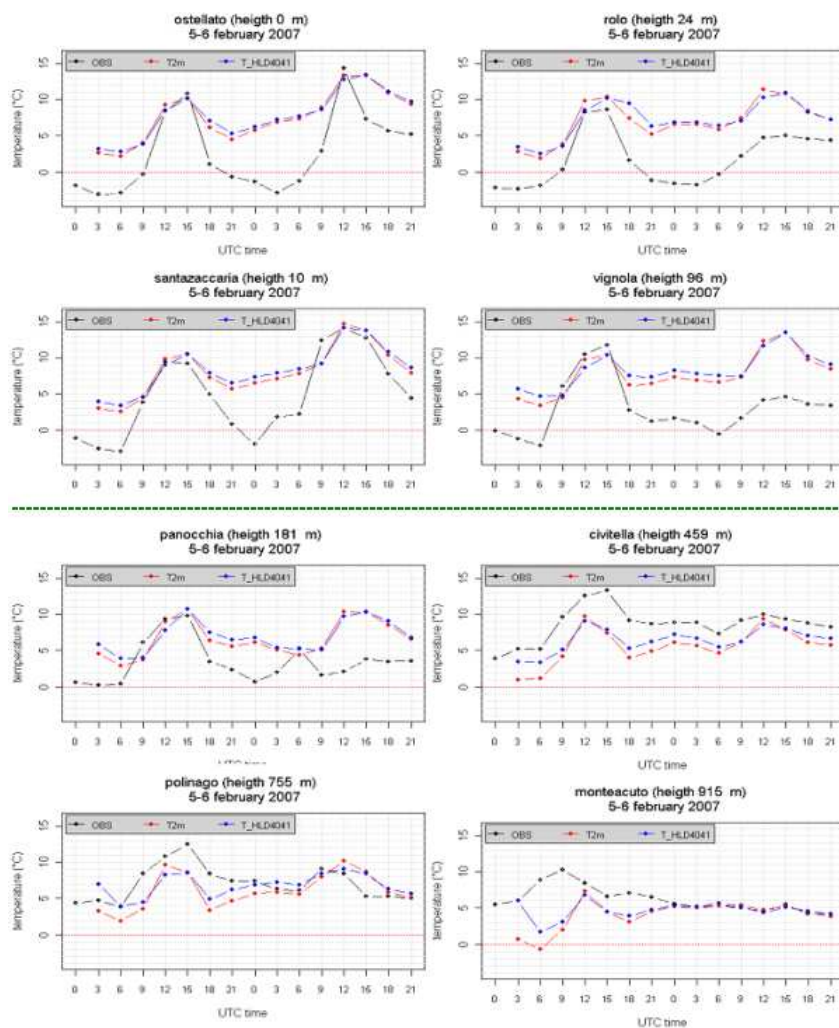


Figure 12: Forecast 2m T and lowermost T (HLD4041) of COSMO-I7 00 UTC (+3h to +45h) and observed temperature in 8 stations at different altitude (<100 m: 4 upper frames,>100 m: 4 lower frames). Observations: black line, COSMO-I7 2m temperature: red line, COSMO-I7 T HLD4041: blue line.

## List of COSMO Newsletters and Technical Reports

(available for download from the COSMO Website: [www.cosmo-model.org](http://www.cosmo-model.org))

### *COSMO Newsletters*

- No. 1: February 2001.
- No. 2: February 2002.
- No. 3: February 2003.
- No. 4: February 2004.
- No. 5: April 2005.
- No. 6: July 2006; Proceedings from the COSMO General Meeting 2005.
- No. 7: May 2008; Proceedings from the COSMO General Meeting 2006.
- No. 8: August 2008; Proceedings from the COSMO General Meeting 2007.

### *COSMO Technical Reports*

- No. 1: Dmitrii Mironov and Matthias Raschendorfer (2001):  
*Evaluation of Empirical Parameters of the New LM Surface-Layer Parameterization Scheme. Results from Numerical Experiments Including the Soil Moisture Analysis.*
- No. 2: Reinhold Schrodin and Erdmann Heise (2001):  
*The Multi-Layer Version of the DWD Soil Model TERRA\_LM.*
- No. 3: Günther Doms (2001):  
*A Scheme for Monotonic Numerical Diffusion in the LM.*
- No. 4: Hans-Joachim Herzog, Ursula Schubert, Gerd Vogel, Adelheid Fiedler and Roswitha Kirchner (2002):  
*LLM - the High-Resolving Nonhydrostatic Simulation Model in the DWD-Project LIT-FASS.*  
*Part I: Modelling Technique and Simulation Method.*
- No. 5: Jean-Marie Bettems (2002):  
*EUCOS Impact Study Using the Limited-Area Non-Hydrostatic NWP Model in Operational Use at MeteoSwiss.*
- No. 6: Heinz-Werner Bitzer and Jürgen Steppeler (2004):  
*Documentation of the Z-Coordinate Dynamical Core of LM.*
- No. 7: Hans-Joachim Herzog, Almut Gassmann (2005):  
*Lorenz- and Charney-Phillips vertical grid experimentation using a compressible non-hydrostatic toy-model relevant to the fast-mode part of the 'Lokal-Modell'*
- No. 8: Chiara Marsigli, Andrea Montani, Tiziana Paccagnella, Davide Sacchetti, André Walser, Marco Arpagaus, Thomas Schumann (2005):  
*Evaluation of the Performance of the COSMO-LEPS System*

- 
- No. 9: Erdmann Heise, Bodo Ritter, Reinhold Schrodin (2006):  
*Operational Implementation of the Multilayer Soil Model*
- No. 10: M.D. Tsyrlnikov (2007):  
*Is the particle filtering approach appropriate for meso-scale data assimilation?*
- No. 11: Dmitrii V. Mironov (2008):  
*Parameterization of Lakes in Numerical Weather Prediction. Description of a Lake Model.*